ELSEVIER

Journal of Organometallic Chemistry 518 (1996) 121–138

Journal of Organometallic Chemistry

A novel method of introducing the $Au_2(PR_3)_2$ (R = Ph, OMe) unit into metal clusters X-ray structures of three complexes containing Au_2Ru_3 cores and of $Ru_6C(\mu\text{-}CO)_2(CO)_{14}\{Au(PPh_3)\}_2$

Michael I. Bruce *, Ernst Horn, Paul A. Humphrey, Edward R.T. Tiekink

Jordan Laboratories, Department of Chemistry, University of Adelaide, Adelaide, S.A. 5005, Australia

Received 27 November 1995

Abstract

The complexes $Ru_3(\mu_3\text{-}C_6H_3R)\{\mu\text{-}P(C_6H_4R\text{-}3)_2\}_2(CO)_6\{Au_2(PPh_3)_2\}$ (R = H (**2**), Me), $Ru_3\{\mu_3\text{-}PPhCH_2PPh(C_6H_4\text{-}2)\}(CO)_8\{Au_2(PR_3)_2\}$ (R = Ph, OMe (**5**)), $Ru_3(\mu_3\text{-}NPh)_n(CO)_{10-n}\{Au_2(PPh_3)_2\}$ (n = 1 (**6**), 2) and $Ru_3(\mu_3\text{-}S)_2(CO)_8\{Au_2(PPh_3)_2\}$ have been obtained from reactions between $[O\{Au(PR_3)\}_3]^+$ (R = Ph, OMe) and the 'parent' Ru_3 clusters; X-ray structural studies of **2**, **5** and **6** show that a CO group has been replaced by an $Au_2(PR_3)_2$ fragment. In contrast, the two $Au(PPh_3)$ groups bridge opposite Ru–Ru bonds in $Ru_6C(\mu\text{-}CO)_2(CO)_{14}\{Au(PPh_3)\}_2$ (**9**; X-ray structure). The known complexes $Os_3(CO)_{11}\{Au_2(PPh_3)_2\}$, and $Os_3H_{2-n}(CO)_{10}\{Au(PPh_3)\}_n$ (n = 1, 2) were obtained from $Os_3(CO)_{12}$ and $Os_3H_2(CO)_{10}$ respectively.

Keywords: Gold; Ruthenium; Clusters; Crystal structure

1. Introduction

There is still much interest in the chemistry of metal cluster complexes which contain $Au(PR_3)$ fragments. This stems from the early work of Lewis and Nyholm [1] some 30 years ago and has continued unabated since then, with periodic invigorations resulting from the recognition of the isolobal properties of H^+ and $[Au(PR_3)]^+$ [2], the development of homonuclear gold cluster chemistry [3], and preparations of so-called 'clusters of clusters', including compounds containing up to 38 atoms described by Teo et al. [4]. Several reviews are available [3,5].

Many reactions leading to the incorporation of one $Au(PR_3)$ fragment into metal clusters have been described [5a,c]. In some cases, repetition of the reaction has given clusters containing two such units. Some years ago, we [6] and later, others [7], described reactions of the trigold-oxonium cation $[O\{Au(PPh_3)\}_3]^+$ with metal cluster hydrides or anions to form a range of complexes containing two, three or four $Au(PPh_3)$ groups. Since then, we have also communicated the use of this cation in the presence of a nucleophile such as acetate or $[Co(CO)_4]^-$ to introduce two $Au(PPh_3)$ groups, or an $Au_2(PPh_3)_2$ moiety, into selected cluster complexes [8].

This paper describes experiments designed to give complexes containing two $Au(PR_3)$ groups, while a following paper [9] will describe complexes containing three such groups. Complexes containing Au_2Ru_3 cores have been reported to show fluxional behaviour in solution, whereby the Au atoms exchange positions in the trigonal pyramidal metal cluster [10]. A series of structurally determined Au_2Ru_3 geometries has been used to map the reaction coordinate of the postulated mechanism for this exchange (a Berry pseudo-rotation process) [11]. The molecular structures of several of the complexes described below further illustrate this feature.

2. Results and discussion

We have investigated the reactions of $[O\{Au(PPh_3)\}_3]^+$ (**1a**) with a number of triruthenium and

* Corresponding author.

PII S0022-328X(96)06195-5

triosmium clusters using [ppn][$Co(CO)_4$] as an agent to remove one of the $Au(PPh_3)$ groups (as $Co\{Au(PPh_3)(CO)_4\}$ and generating '$Au_2(PPh_3)_2$' in situ. The reactions were carried out in tetrahydrofuran at room temperature and generally took less than an hour to complete. Work up of the reaction mixture by thin layer chromatography allowed easy separation of $Co\{Au(PPh_3)\}(CO)_4$, with the major product(s) being contained in well-resolved band(s) at lower R_f values. Other anions, such as chloride and acetate, have also been used with similar results. Isolated yields of the pure gold–ruthenium or –osmium cluster complexes ranged from 21–80%. Characterisation of the various complexes was achieved by a combination of elemental analysis and the usual spectroscopic methods (see Tables 1 and 2 and the Experimental section). In general, the FAB mass spectra contained parent ions, although some contained ions at higher mass formed by addition of an $Au(PPh_3)$ group to M^+, similar to those described earlier [12] (see Table 2). Selected complexes have been fully characterised by single-crystal X-ray structure determinations.

In this way, we have found that replacement of either one CO group or two cluster-bound H atoms (if present) by the $Au_2(PPh_3)_2$ unit occurred to give novel derivatives (Scheme 1), several of which have been structurally characterised (see below). We have also used the $[O\{Au[P(OMe)_3]\}_3]^+$ cation (**1b**) in some of these reactions. With the exception of obvious changes in the ^1H NMR spectra, no significant differences in the products were found. In the account that follows, we have chosen to represent complexes containing adjacent $Au(PR_3)$ groups (i.e. Au–Au bonded) by $Au_2(PR_3)_2$, while in complexes with separated (non-bonded) $Au(PR_3)$ groups, the formulation $\{Au(PR_3)\}_2$ has been employed.

Thus, from reactions between **1a** and $Ru_3(\mu_3\text{-}C_6H_4)(\mu\text{-}PPh_2)_2(CO)_7$, the corresponding hexacarbonyl (**2**) was obtained as a dark purple crystalline solid. The related complex $Ru_3(\mu_3\text{-}C_6H_3Me)\{\mu\text{-}P(C_6H_4Me\text{-}3)_2\}_2(CO)_6\{Au_2(PPh_3)_2\}$ (**3**) was obtained similarly, both being isolated in about 70% yield. Spectroscopic data for **2** and **3** were in accord with these formulations, only three terminal $\nu(CO)$ bands being found in their IR spectra (Table 1); individual characteristic resonances in their ^1H NMR spectra are mentioned where appropriate. Thus for **3**, three Me resonances at δ 1.87, 2.13 and 2.18 (intensity ratio 1:2:2) could be assigned to the Me groups of the $\mu_3\text{-}C_6H_3Me$ and the two $P(C_6H_4Me)_2$ ligands respectively. The X-ray crystal structure of **2** confirmed that the two $Au(PR_3)$ groups were adjacent.

A similar reaction between **1a** and $Ru_3\{\mu_3\text{-}PPhCH_2PPh(C_6H_4\text{-}2)\}(CO)_9$ also resulted in replacement of a CO group by the $Au_2(PPh_3)_2$ fragment to give the purple complex **4**. In this complex, only three terminal $\nu(CO)$ bands were found, while the ^1H NMR spectrum contained two multiplets at δ 2.89 and 3.65 for the CH_2 groups of the bridging phosphido–phosphine ligand. There were no significant differences in yields when [ppn][OAc] or [ppn]Cl were used as the accompanying nucleophiles: one-third of the gold was separated as the compounds $Au(OAc)(PPh_3)$ or $AuCl(PPh_3)$ respectively. When $[O\{Au[P(OMe)_3]\}_3][BF_4]$ was used as the $Au_2(PR_3)_2$ source, the complex $Ru_3\{\mu_3\text{-}PPhCH_2PPh(C_6H_4\text{-}2)\}(CO)_8\{Au_2[P(OMe)_3]_2\}$ (**5**) was obtained in 75% yield. The IR spectrum contains four terminal $\nu(CO)$ bands, while in its ^1H NMR spectrum, the OMe protons resonated as two doublets at δ 3.55 and 3.83. The X-ray crystal structure of **5** is described below.

Reactions with the μ_3-NPh complexes $Ru_3(\mu_3\text{-}NPh)_n(CO)_{11-n}$ ($n = 1, 2$) with **1a** afforded the corresponding complexes $Ru_3(\mu_3\text{-}NPh)_n(CO)_{10-n}\{Au_2(PPh_3)_2\}$ as red ($n = 1$, (**6**)) and orange ($n = 2$, (**7**)) crystalline solids respectively. Their IR spectra contain five and six terminal $\nu(CO)$ bands respectively; the ^1H

Table 1
Some complexes containing $Au(PR_3)$ fragments

No	Complex	Colour	M.p. (°C) [a]	Analyses: found/calc.		
				C	H	N
2	$Ru_3(\mu\text{-}C_6H_4)(\mu\text{-}PPh_2)_2(CO)_6\{Au_2(PPh_3)_2\}$	dark purple	> 150 dec	47.47/47.10	3.37/2.96	
3	$Ru_3(\mu_3\text{-}C_6H_3Me)\{\mu\text{-}P(C_6H_4Me\text{-}4)_2\}_2(CO)_6\{Au_2(PPh_3)_2\}$	purple	> 150 dec	48.80/48.51	3.59/3.38	
4	$Ru_3\{\mu_3\text{-}PPhCH_2PPh(C_6H_4)\}(CO)_8\{Au_2(PPh_3)_2\}$	red	198–200	42.72/43.19	2.64/2.65	
5	$Ru_3\{\mu_3\text{-}PPhCH_2PPh(C_6H_4)\}(CO)_8\{Au_2[P(OMe)_3]_2\}$	red-purple	200–203	26.80/26.86	2.32/2.32	
6	$Ru_3(\mu_3\text{-}NPh)(CO)_9\{Au_2(PPh_3)_2\}$	dark red	> 150 dec	39.02/39.14	2.26/2.25	0.90/0.90
7	$Ru_3(\mu_3\text{-}NPh)_2(CO)_8\{Au_2(PPh_3)_2\}$	orange	> 150 dec	41.6/41.3	2.8/2.5	2.0/1.7
8	$Ru_3(\mu_3\text{-}S)_2(CO)_8\{Au_2(PPh_3)_2\}$	red	> 150 dec	34.97/35.00	2.01/2.00	
9	$Ru_6C(CO)_{16}\{Au(PPh_3)\}_2$	red	278–280	31.35/31.69	1.50/1.54 [b]	
10	$Os_3(CO)_{11}\{Au_2(PPh_3)_2\}$	orange	155–156 dec	31.28/31.41	1.71/1.68	
11	$Os_3(CO)_{11}\{Au_2[P(OMe)_3]_2\}$	orange	> 150 dec	13.52/13.43	1.20/1.19	
12	$Os_3(CO)_{10}\{Au(PPh_3)\}_2$	dark green	204–207 dec			
13	$Os_3(\mu\text{-}H)(CO)_{10}\{Au(PPh_3)\}$	dark green		24.80/25.65	1.32/1.23	
14	$Os_3(\mu\text{-}H)_2(CO)_9(PPh_3)\{Au(PPh_3)\}_2$	golden yellow		37.14/37.73	2.44/2.36	

[a] dec = decomposed. [b] $0.5CH_2Cl_2$ solvate.

Table 2
Spectroscopic properties of some Au–Ru and Au–Os complexes

No.	IR ν(CO) (cm^{-1}) (solvent)	Highest ion [a]	Partial mass spectra (FAB)/rel. intensities (%)												
			$[M-nCO]^{+}$ [b]												
			0	1	2	3	4	5	6	7	8	9	AuP_2	AuP	Other ions
2	1979vs(br), 1946m, 1927m(br) (C_6H_{12})	M	5	28	6	3	9	17	4				100	88	$[M'-P-Ph]^+$, 24; $[M'-P-2Ph]^+$, 13;
		M−P		3	4	8	22	25	35						$[M'-AuP-Ph]^+$, 35; $[M'-AuP-2Ph]^+$, 27
3	1977vs(br), 1945m, 1927m(br) (C_6H_{12})	M	2	5									100	38	$[M-6CO-PPh_3-C_6H_4Me]^+$, 4;
		M−P		2			3		10						$[M-6CO-AuP-C_6H_4Me]^+$, 7
4	2033m, 1980vs(br), 1925m(br) (CH_2Cl_2)	M	3	3	2	6	3	2	3	3	4		100	65	$[M+AuP]^+$, 3; $[M-AuP-CO]^+$, 6
5	2030m, 1986vs, 1977vs, 1934w(br) (CH_2Cl_2)	M+AuP	3	2	5	7	5	2							$[M-AuP]^+$, 11; $[M-AuP-CO]^+$, 14
		M+Au		1	2	3	3	6	3						
		M	5	7	6	53	20	15	22	11	6		43	100	
		M−P	5	5	5	9	8	12	14						
6	2052w, 2028vs, 2014vs, 1980(sh), 1972m, 1960s, 1952(sh) (C_6H_{12})	M	63	37	43	25	37	100	25	55	72	61	100	50	$[M-8CO-N]^+$, 41; $[M-9CO-Ph]^+$, 50
7	2066s, 2049vs, 1993vs, 1988vs, 1972m, 1966s, 1912m (C_6H_{12})	M	1	8	7		6	3	5	4	18		63	100	$[M-8CO-Ph]^+$, 5
8	2073s, 2053vs, 2005s, 1990vs, 1974m, 1924m (C_6H_{12})	M	6	13	1	2	23	1	3	6	21		57	100	$[M-8CO-Ph]^+$, 6
9	2067w, 2049s, 2017vs, 1965w, 1822m (br) (CH_2Cl_2)	M	19	3									94	100	$[M-AuP]^+$, 3; $[M-2AuP]^+$, 15
10	2097m, 2048s, 2015vs, 1997(sh), 1978w, 1966w, 1930(sh), 1918w (CH_2Cl_2) [c]	M	4	2	3	1		2	2	3			100	44	
11	2101m, 2051s, 2019vs, 2003(sh), 1979w, 1969w, 1936(sh), 1922w (CH_2Cl_2)	M	15	9	25	39	14	11	15	21			100		
12	2070w, 2017s, 1982m, 1955w, 1944m (CH_2Cl_2) [d]	M	7	10	3	2	7	4	10				100	41	$[M-2CO-AuP]^+$, 10
13	2090w, 2047vs, 2041s, 2008s, 1997s, 1980s (hexane) [e]	M	66	11	10	8	23	8	31	12	18		81	100	
14	2075vw, 2043w, 1998vs, 1991(sh), 1962w(br), 1923w, 1918w (C_6H_{12})	M	4	1	1	1		1					100	69	$[M+AuP]^+$, 1; $[M+Au]^+$, 2; $[M-C_6H_4-nCO]^+$, 2($n=0$), 2(3), 13(8); $[M-C_6H_6-AuP]^+$, 49

[a] P = PPh_3 or $P(OMe)_3$ as appropriate; M′ = M−6CO. [b] M relates to highest ion series. [c] Ref. [15] 2111m, 2067m, 2031s, 2020(sh), 2000m, 1978(sh), 1955(sh), 1931(sh) (CH_2Cl_2). [d] Ref. [15] 2067w, 2012s, 1977m, 1965w, 1937m. [e] Ref. [18] 2090w, 2047s, 2040m, 2008s, 1996m, 1977m (hexane).

NMR spectra were uninformative, containing only the expected bands. The X-ray structure of **6** confirmed the anticipated structure, in which the μ_3-CO ligand has been replaced by an $Au_2(PPh_3)_2$ group.

Use of [ppn]X (X = Cl, OAc or $Co(CO)_4$) in reactions between **1a** and $Ru_3(\mu_3\text{-}S)_2(CO)_9$ again resulted in no difference in product, although the yields of red $Ru_3(\mu_3\text{-}S)_2(CO)_8\{Au_2(PPh_3)_2\}$ (**8**) varied from 21 (X = Cl) to 69% (X = $Co(CO)_4$). Related complexes have been obtained from $Ru_3(\mu\text{-}H)_2(\mu_3\text{-}S)(CO)_9$ and the related anion and structurally characterised [13]; however, we were unable to obtain suitable X-ray quality crystals to enable the molecular structures of **7** or **8** to be determined. The presence of two μ_3-ligands on either side of an open Ru_3 cluster suggests that the two $Au(PPh_3)$ units may either bridge the two Ru–Ru edges, or bridge only one edge as an $Au_2(PPh_3)_2$ unit.

In the series of reactions of ruthenium complexes examined here, only that of **1a** with $Ru_6C(CO)_{17}$ afforded a complex containing two isolated $Au(PPh_3)$ groups, as revealed by the X-ray structure of $Ru_6C(\mu\text{-}CO)_2(CO)_{14}\{Au(PPh_3)\}_2$ (**9**), a red crystalline solid obtained in 47% yield as the $0.5CH_2Cl_2$ solvate. This complex has been reported briefly, together with other related phosphine derivatives, as having been obtained from reactions between $[Au(PR_3)]^+$ (R = Me, Et, Ph; R_3 = $MePh_2$) and $[Ru_6C(CO)_{16}]^{2-}$ [14]. The IR spectrum contains four terminal ν(CO) bands, together with an absorption at 1822 cm^{-1} assigned to a μ-CO ligand.

Reactions of $Os_3(CO)_{12}$ with $[O\{Au(PR_3)\}_3]^+$ (R =

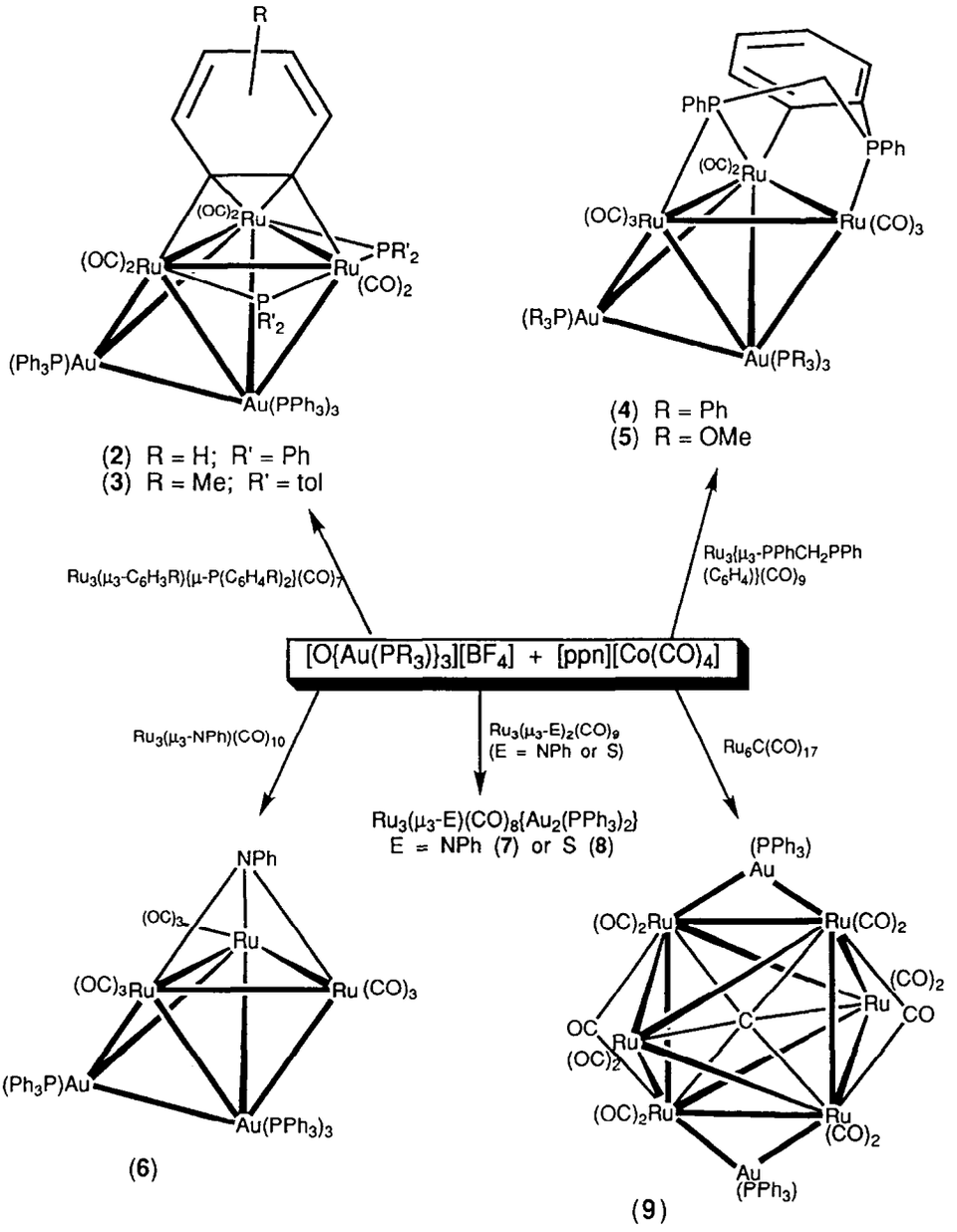

Scheme 1.

Ph or OMe) also proceeded readily at room temperature. The orange products, obtained in 53–71% yield, were identified as $Os_3(CO)_{11}\{Au_2(PR_3)_2\}$ (R = Ph (**10**), OMe (**11**)) by analysis and spectroscopically. In this series of reactions, [ppn]X (X = Cl, OAc and $Co(CO)_4$) were used as accompanying nucleophiles: the compounds $AuX(PR_3)$ were also isolated, together with a white precipitate of [ppn][BF_4]. The ^{1}H NMR spectrum of **11** contained a doublet at δ 3.79 for the OMe protons. Complex **10** has been characterised previously by an X-ray structure determination [15,16]. As reported in the Experimental section, the IR ν(CO) spectrum of our product differs from that reported earlier [15].

In contrast, with $Os_3(CO)_{11}$(NCMe) and **1a** the reaction gave several products, but only $Co\{Au(PPh_3)\}(CO)_4$ and green $Os_3(CO)_{10}\{Au(PPh_3)\}_2$ (**12**; 51%) have been isolated and identified. The PEt_3 analogue was described before in an account which details the extensive relationships that exists between these complexes [15]. The molecular core consists of an equilateral triangle of Os atoms, the shorter edge of which is bridged by two $Au(PEt_3)$ units; there is no interaction between the two Au atoms, whch are separated by 4.304(2) Å. This complex is therefore isolobal with the dihydride $Os_3(\mu\text{-}H)_2(CO)_{10}$.

The purple colour of the latter complex was immediately discharged upon addition of the gold reagent, the solution becoming greenish-brown. Work up gave **12** (8%) and the hydrido–gold complexes $Os_3(\mu\text{-}H)(CO)_{10}\{Au(PPh_3)\}$ (**13**; 15%) [15] and $Os_3(\mu\text{-}H)_2(CO)_9(PPh_3)\{Au(PPh_3)\}_2$ (**14**). Complex **13** has been obtained previously from reactions of the dihydride with $AuMe(PPh_3)$ [17] and of [ppn][$Os_3(\mu\text{-}H)(CO)_{11}$] with $AuCl(PPh_3)$ [15,18]. Golden-yellow **14** was tentatively identified in the usual way, the ^{1}H NMR spectrum containing two resonances in the high field region at δ − 17.04 and − 7.01, assigned to μ-H and terminal H ligands respectively. The FAB mass spectrum contained a strong M^+ ion. The complex may be related to $Os_3H(\mu\text{-}H)(CO)_{10}(PPh_3)$ [19], with one of the CO groups replaced by two $Au(PPh_3)$ groups, although we cannot determine whether there is an Au–Au bond in this product.

Table 3
Selected bond lengths (Å) for complexes **2**, **5** and **6** and their 'parent' complexes (from Refs. [20–22])

$Ru_3(\mu_3\text{-}C_6H_4)(\mu\text{-}PPh_2)_2(CO)_6\{Au_2(PPh_3)_2\}$ (**2**) [a]		
		Parent complex
Ru(1)–Ru(2)	2.847(4)	2.776(1)
Ru(1)–Ru(3)	2.831(5)	2.759(1)
Ru(2)–Ru(3)	3.012(4)	2.956(1)
Ru(1)–P(3)	2.300(9)	2.267(2)
Ru(2)–P(3)	2.34(1)	2.334(2)
Ru(2)–P(4)	2.37(1)	2.319(2)
Ru(3)–P(4)	2.278(9)	2.361(2)
Ru(1)–C(1)	2.29(3)	2.303(6)
Ru(1)–C(2)	2.35(2)	2.353(6)
Ru(2)–C(2)	2.16(2)	2.127(6)
Ru(3)–C(1)	2.09(2)	2.135(6)
C(1)–C(6)	1.39(3)	1.40
$Ru_3\{\mu_3\text{-}PhCH_2PPh(C_6H_4)\}(CO)_8\{Au_2[P(OMe)_3]_2\}$ (**5**)		
Ru(1)–Ru(2)	2.915(2)	2.8250(7)
Ru(1)–Ru(3)	2.991(2)	2.8962(7)
Ru(2)–Ru(3)	3.054(2)	2.8618(7)
Ru(1)–P(3)	2.330(4)	2.303(1)
Ru(2)–P(4)	2.386(4)	2.359(1)
Ru(3)–P(3)	2.317(4)	2.349(1)
Ru(3)–C(2)	2.10(1)	2.170(4)
$Ru_3(\mu_3\text{-}NPh)(CO)_9\{Au_2(PPh_3)_2\}$ (**6**)		
Ru(1)–Ru(2)	2.730(2)	2.735(1), 2.734(1) [b]
Ru(1)–Ru(3)	2.909(1)	2.750(1), 2.760(1)
Ru(2)–Ru(3)	2.821(1)	2.741(1), 2.754(1)
Ru(1)–N(1)	2.083(9)	2.055(4), 2.055(4)
Ru(2)–N(1)	2.063(9)	2.053(4), 2.060(4)
Ru(3)–N(1)	2.057(8)	2.053(4), 2.054(4)

[a] Dihedral angle C_6H_4–Ru_3 70.5°; parent complex 65.2°.
[b] Values for two independent molecules given.

Table 4
Selected bond lengths (Å) for **9** and $Ru_6C(CO)_{17}$ [23]

	9	Parent (av.) [a]
Au(1)–Ru(1)	2.785(2)	
Au(1)–Ru(2)	2.753(2)	
Au(1)–P(1)	2.281(6)	
Ru(1)–Ru(2)	3.046(3)	2.898(3) (I)
Ru(1)–Ru(3)	2.941(3)	2.893 (IIa)
Ru(2)–Ru(3)	2.874(3)	2.885 (IIb)
Ru(1)–C(1)	2.075(2)	2.05 (all forms)
Ru(2)–C(1)	2.076(2)	
Ru(3)–C(1)	2.023(2)	
Ru(1)–C(11)	2.09(3)	
Ru(2)–C(11)	2.04(3)	

[a] Values for forms I, IIa and IIb given as appropriate.

2.1. Molecular structures

The molecular structures of **2**, **5**, **6** and **9** have been determined and important structural parameters are given

Table 5
Bond lengths (Å) for the $Ru_3Au_2(PR_3)_2$ fragments in complexes **2**, **5** and **6**

	2	**5**	**6**
Au(1)–Au(2)	3.032(2)	2.763(5)	2.955(1)
Au(1)–Ru(1)	2.835(3)	2.845(1)	2.784(1)
Au(1)···Ru(2)	4.830(3)	4.810(1)	4.531(2)
Au(1)–Ru(3)	2.690(3)	2.900(1)	2.811(1)
Au(2)–Ru(1)	2.845(3)	2.874(1)	2.937(1)
Au(2)–Ru(2)	3.094(3)	3.070(1)	2.804(1)
Au(2)–Ru(3)	2.728(3)	2.742(1)	2.828(1)
Au(1)–P(1)	2.282(9)	2.266(5)	2.300(3)
Au(2)–P(2)	2.327(8)	2.253(5)	2.309(3)
Ru(1)–Ru(2)	2.847(4)	2.915(2)	2.730(2)
Ru(1)–Ru(3)	2.831(5)	2.991(2)	2.909(1)
Ru(2)–Ru(3)	3.012(4)	3.054(2)	2.821(1)

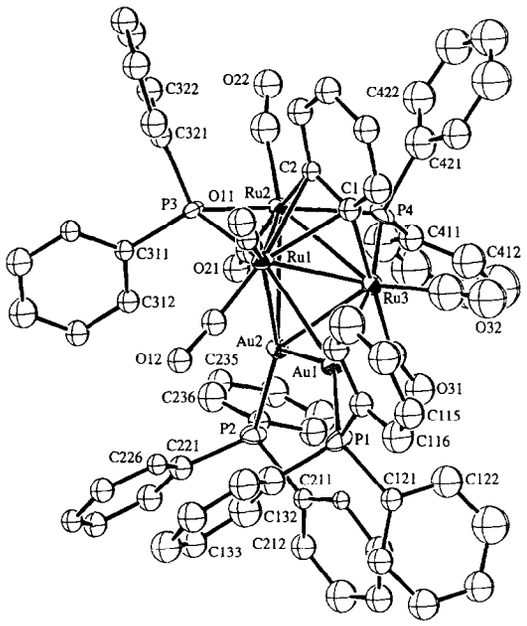

Fig. 1. Molecular structure and crystallographic numbering scheme for $Ru_3(\mu_3\text{-}C_6H_4)(\mu\text{-}PPh_2)_2(CO)_6\{Au_2(PPh_3)_2\}$ (**2**).

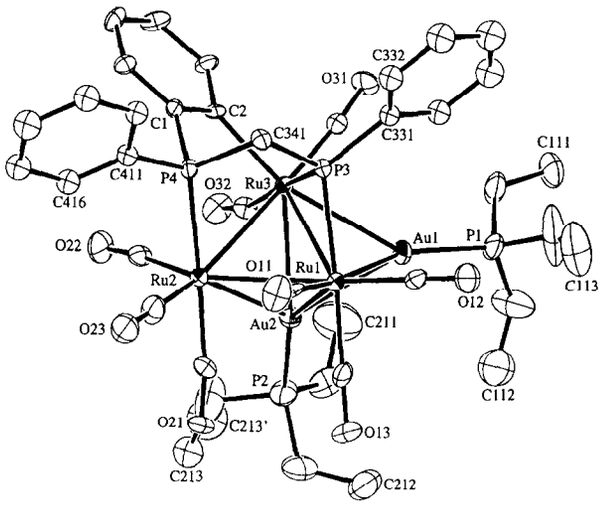

Fig. 2. Molecular structure and crystallographic numbering scheme for the cluster in $Ru_3\{\mu_3\text{-}PPhCH_2PPh(C_6H_4\text{-}2)\}(CO)_8\{Au_2(P(OMe)_3)_2\}\cdot CH_2Cl_2$ (**5**).

in Tables 3 and 4. All three Ru_3 derivatives contain approximately trigonal pyramidal Au_2Ru_3 cores (Table 5), as found for 16 related complexes in the earlier study [11]. In the following account, some comparisons with the 'parent' complexes are also given.

2.1.1. $Ru_3(\mu_3\text{-}C_6H_4)(\mu\text{-}PPh_2)_2(CO)_6\{Au_2(PPh_3)_2\}$ (2)

As can be seen from Fig. 1, the benzyne ligand remains attached to the Ru_3 face; the equatorial Ru atoms interact with the C_6H_4 group in η^1 and η^2 modes, the apical Ru in an η^1 mode. The two PPh_2 groups bridge the Ru(1)–Ru(2) and Ru(2)–Ru(3) vectors. The $Au_2(PPh_3)_2$ group is attached via Au(2) to all three Ru atoms (range 2.728(4)–3.094(3) Å) and more strongly to Ru(1) and Ru(3) via Au(1) (2.835(3), 2.690(4) Å respectively); there is no obvious reason for the dissimilarity in Au–Ru bond distances. Comparison with the parent complex [20] shows that all Ru–Ru distances are longer in **2** (2.897 (av.) vs. 2.830 Å). The Ru–C distances to the benzyne ligand appear to indicate a strengthening of the σ-bonds at the expense of the π-bonds; however, this trend is partially obscured by an increase in asymmetry of bonding of the C(1)–C(2) unit to the Ru_3 triangle when the $Au_2(PPh_3)_2$ fragment is present.

2.1.2. $Ru_3\{\mu_3\text{-}PPhCH_2PPh(C_6H_4\text{-}2)\}(CO)_8\{Au_2[P(OMe)_3]_2\}$ (5)

Fig. 2 shows a plot of this complex, which was characterised as a CH_2Cl_2 solvate. The metallated phosphido–phosphine ligand is attached to the apical Ru(2) via P(4) (the phosphine), while P(3) (the phosphide) bridges the Ru(1)–Ru(3) vector. The Au–Ru bonds fall in the range 2.742(1)–3.070(1) Å, the shortest bond being to Ru(3) which also bears the σ-bonded C_6H_4 group (Ru(3)–C(2) 2.10(1) Å). Again, there is an expansion of the Ru_3 triangle in **5** (2.915(2)–3.054(2) Å, av. 2.987 Å) when compared with the parent complex (2.8250(7)–2.8962(7) Å, av. 2.861 Å) [21]. Other bonds are comparable, with the exception of Ru(3)–C(2) (2.10(1) Å in **5** vs. 2.170(4) Å in the parent).

2.1.3. $Ru_3(\mu_3\text{-}NPh)(CO)_9\{Au_2(PPh_3)_2\}$ (6)

Fig. 3 shows that this complex contains the Au_2Ru_3 trigonal bipyramid found in the previous examples, with the Ru_3 face capped by the NPh group. In the precursor, one of the CO groups caps the opposite side of the

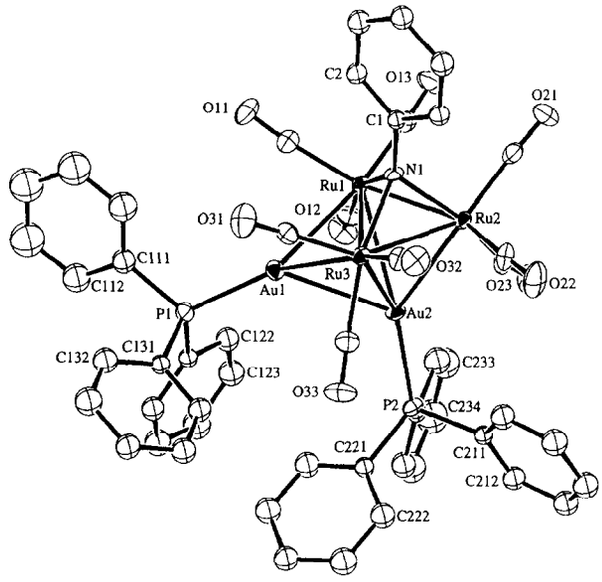

Fig. 3. Molecular structure and crystallographic numbering scheme for $Ru_3(\mu_3\text{-}NPh)(CO)_9\{Au_2(PPh_3)_2\}$ (**6**).

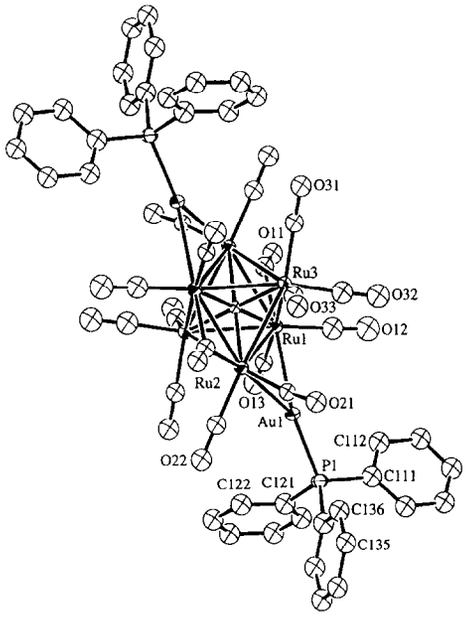

Fig. 4. Molecular structure and crystallographic numbering scheme for the cluster in $Ru_6C(\mu\text{-}CO)_2(CO)_{14}\{Au(PPh_3)\}_2 \cdot 0.5CH_2Cl_2$ (**9**).

face [22]. In the formation of **6**, the $Au_2(PPh_3)_2$ group (a 2e donor) has replaced this CO ligand, but the pronounced tendency for metal–metal bond formation has resulted in condensation to the observed trigonal bipyramid. The nine remaining CO groups are terminally bound, three to each Ru atom. The Au–Ru separations range between 2.784(1) and 2.937(1) Å, while within the Ru_3 triangle, the average Ru–Ru separation of 2.820 Å again shows an increase when compared with the values of 2.742, 2.749 Å found for the two independent molecules of the parent complex [18]. Attachment of the $Au_2(PPh_3)_2$ unit also results in the equatorial Ru(1)–Ru(3) vector (2.909(1) Å) in the Ru_3Au_2 trigonal bipyramid being longer than the two Ru(eq)–Ru(ap) distances.

2.1.4. $Ru_6C(\mu\text{-}CO)_2(CO)_{14}\{Au(PPh_3)\}_2$ (9)

In this complex, obtained as a hemi-CH_2Cl_2 solvate, the structure (Fig. 4 and Table 5) is based on that of the parent $Ru_6C(CO)_{17}$ [23], the two $Au(PPh_3)$ groups are as far apart as possible, bridging opposite edges (Ru(1)–Ru(2) and Ru(1′)–Ru(2′)) of the Ru_6 octahedron. The other two equatorial edges (Ru(1)–Ru(2′) and Ru(2)–Ru(1′)) are bridged by CO ligands to give a symmetrical structure. In contrast, the $PMePh_2$ complex contains a slightly distorted octahedron with the central carbon atom at a crystallographic centre of symmetry [14]. While the Au–Ru and Au–P bonds are experimentally identical in the two complexes, there is a considerable disparity between the two sets of Ru–Ru distances. Thus in **9**, the three separations Ru(1)–Ru(2), Ru(1)–Ru(3) and Ru(2)–Ru(3) are 3.046(3) Å, 2.941(3) Å and 2.874(3) Å respectively (av. 2.954 Å), while in the $PMePh_2$ complex the corresponding distances are in the range 2.758(1)–2.950(1) Å, with an average of 2.870 Å. It has previously been noted that there is no correspondence between Ru–Ru separation and the presence or absence of bridging ligands in the three structural forms of $Ru_6C(CO)_{17}$ that have been identified [23]. However, the entire range of distances spanned lies between 2.803(1) and 2.988(1) Å, with an average value of 2.892 Å. This is 0.064 Å shorter than that found in **9**, but 0.022 Å longer than in the $PMePh_2$ complex [14]. Of interest is that the Ru_6 octahedron is flattened, the Ru(3)–C(1) distance being 0.54 Å shorter than the Ru(eq)–C(1) distances; a similar difference (0.43 Å) was also found in the $PMePh_2$ complex.

2.2. FAB mass spectra

As reported earlier [12], fast atom bombardment (FAB) mass spectrometry has proved very useful for the identification of involatile, high molecular weight metal cluster complexes. In the present instance, all complexes gave well resolved spectra, with the molecular ion prominent (Table 2). Fragmentation is by loss of CO ligands and in several cases, loss of $Au(PPh_3)$ groups or fragments thereof. The dominant peaks in all spectra, however, are the ions $[Au(PR_3)_n]^+$ (R = Ph or OMe, $n = 1$ or 2).

For **6**, strong peaks at m/z 1328 and 1237 were assigned to $[M - 8CO - N]^+$ and $[M - 9CO - Ph]^+$ respectively; loss of Ph (or C_6H_4Me) groups was also found in the spectra of **2** and **3**. Aggregate ions of the type $[M + Au(PR_3)]^+$ were found in the spectra of **5** and **14** and may be considered to be isolobal with the $[M + H]^+$ ions commonly found in FAB mass spectra of organic and some organometallic molecules [12].

Table 6
$^{31}P\{^1H\}$ NMR data for some Au_2Ru_3 complexes [a]

Complex	Temperature	δ(PAu)	Other signals
$Ru_3(\mu_3\text{-}C_6H_4)(\mu\text{-}PPh_2)_2(CO)_6\{Au_2(PPh_3)_2\}$ (**2**)	r.t.	61.6, 67.1	104.0, 191.2 (2 × PPh_2)
$Ru_3\{\mu_3\text{-}PPhCH_2PPh(C_6H_4)\}(CO)_8\{Au_2(PPh_3)_2\}$ (**4**)	r.t.	62.9, 63.3	0.7 (d, J(PP) = 96 Hz, PPh); 152.1 (d, J(PP) = 96 Hz, μ-PPh)
$Ru_3(\mu_3\text{-}NPh)(CO)_9\{Au_2(PPh_3)_2\}$ (**6**)	205 K	64.5	
$Ru_3(\mu_3\text{-}NPh)_2(CO)_8\{Au_2(PPh_3)_2\}$ (**7**)	r.t.	63.1	
$Ru_3(\mu_3\text{-}S)_2(CO)_8\{Au_2(PPh_3)_2\}$ (**8**)	r.t.	64.7	
$Os_3(CO)_{10}\{Au(PPh_3)\}_2$ (**12**)	r.t.	81.3	

[a] In CH_2Cl_2; external reference 0.01 M H_3PO_4–0.1 M HCl in D_2O (δ 0.8).

2.3. ^{31}P NMR spectra

Table 6 lists the ^{31}P NMR spectra obtained for several of the complexes described above. The chemical shifts for the Au–PR_3 groups attached to an Ru cluster are usually between δ 56–67, as found previously for $Ru_3(\mu_3\text{-}PPhCH_2PPh_2)(CO)_9\{Au(PPh_3)\}$ (δ 68.7) [24], $Ru_3(\mu\text{-}H)(\mu_3\text{-}S)(CO)_9\{Au(PPh_3)\}$ (δ 62.8) [13a], $Ru_3(\mu_3\text{-}S)(CO)_9\{Au_2(PPh_3)_2\}$ (δ 64.4) [13a] and $Ru_4(\mu_3\text{-}H)(\mu\text{-}H)(CO)_{12}\{Au_2(PPh_3)_2\}$ (δ 58.7) [25]. The presence of only one signal indicates that the two $Au(PR_3)$ groups are rendered equivalent by rapid exchange between the two structurally inequivalent sites. As mentioned above, this process probably involves a Berry-type rearrangement of the Au_2Ru_3 metal cores via a square pyramidal intermediate. That this process is a facile one is shown by the observation of a single ^{31}P resonance for **6** even at 205 K. However, for **2**, two signals at δ 61.6 and 67.1 are found, together with two other resonances at δ 104.0 and 191.2, which are assigned to the two PPh_2 groups. Similarly, in the spectrum of **4**, two resonances at δ 62.9 and 63.3 are observed; the ^{31}P resonances of the $P^APhCH_2P^BPh(C_6H_4)$ ligand are found at δ 152.1 (P^A) and 0.7 (P^B), compared with values of δ 117.3 and 2.9 found for $Ru_3\{\mu_3\text{-}PPhCH_2PPh(C_6H_4)\}(CO)_9$ [21a]. In **2** and **4**, the presence of two Au–PPh_3 resonances results from the asymmetry in the Ru_3 parts of the clusters, which do not possess any plane of symmetry. The presence of two PPh_2 resonances in the spectrum of **2** suggests that the $\mu_3\text{-}C_6H_4$ is no longer undergoing a rapid (on the NMR time-scale) rotation about the Ru_3 triangle, as has been observed in the precursor [26]. Further comparisons of the various processes occurring in non-rigid cluster carbonyls containing functional ligands and their $Au(PR_3)$ derivatives are desirable.

3. Conclusions

This paper has described the use of the $[O\{Au(PR_3)\}_3]^+$ (R = Ph, OMe) reagents as sources of the $Au_2(PR_3)_2$ fragment in reactions with a range of trinuclear ruthenium carbonyl complexes. The reactions are carried out in the presence of an anionic nucleophile ($X^- = Cl^-$, OAc^- or $[Co(CO)_4]^-$) which serves to remove one-third of the gold as $AuX(PR_3)$. Earlier studies have shown that treatment of poly-gold clusters with nucleophiles resulted in loss of an $Au(PR_3)$ fragment [27]; in the present case, we have not detected the trigold clusters, although in some cases these are formed by reaction of mono- or di-gold clusters with the trigoldoxonium cation.

With simple trinuclear osmium carbonyls, the reagent results in the formation of mono- and di-gold triosmium clusters, which have been obtained previously by other related routes [15]. Thus, efficient syntheses of $Os_3(CO)_{11}\{Au_2(PR_3)_2\}$ were achieved with both the PPh_3 and $P(OMe)_3$ derivatives. With the dihydride $Os_3H_2(CO)_{10}$, mixtures of $Os_3H(CO)_{10}\{Au(PPh_3)\}$ and $Os_3(CO)_{10}\{Au(PPh_3)\}_2$ were obtained, together with the new hydride $Os_3(\mu\text{-}H)_2(CO)_9(PPh_3)\{Au(PPh_3)\}_2$ (**14**), presumably formed by abstraction of PPh_3 by the Os_3 complex and addition of the digold fragment.

The pattern of substitution is as expected for a two-electron donor, i.e. two H atoms or a CO group. The high tendency for Au–Au bond formation ('aurophilicity') [28], however, means that, in most cases, it is the $Au_2(PR_3)_2$ unit which adds to the clusters, on the opposite side of the Ru_3 cluster from that occupied by the μ_3-capping ligand. Solution studies have shown that the Au–Au bond is readily cleaved with formation of complexes (or intermediates) containing two separated $Au(PR_3)$ groups [10]. This comment is particularly pertinent to the Ru_6 cluster **9**. The structures of this complex and its $PMePh_2$ analogue [14] are similar. The latter shows temperature-dependent ^{31}P NMR spectra, indicating the presence of two isomers of which, it is suggested, one has the solid-state structure and the other contains an $Au_2(PR_3)_2$ unit with an Au–Au bond, as found in the related species $Ru_5WC(CO)_{17}\{Au_2(PEt_3)_2\}$ [14]. Not surprisingly, the chelating phosphine in $Ru_6C(\mu\text{-}CO)_3(CO)_{13}\{Au_2(\mu\text{-}dppm)\}$ keeps the two Au atoms in close contact (2.863(1) Å) as they cap one of the Ru_3 faces of the Ru_6 octahedron [29].

The presence of Au–Au bonds in the Au_2Ru_3 clusters described above indicates that the well-known isolobal relationship between $Au(PR_3)$ and H [30] does not seem to hold in these clusters. In polyhydrido clusters the H atoms are generally found to bridge separate edges or cap separate faces. In the formation of tye digold derivatives, the first $Au(PR_3)$ unit caps an Ru_3 face, while the second caps an $AuRu_2$ face, so that Au–Au bonds are formed. The formal isolobal analogues of these complexes would be cluster complexes of molecular H_2, but so far none have been identified, although their mononuclear counterparts have been known since 1984 [31].

The structural consequences of replacement of a CO by the $Au_2(PR_3)_2$ fragment are generally an expansion of the triangular Ru_3 part of the Au_2Ru_3 core. Others have commented upon the geometries of this core and their relationship with the reaction coordinate of the Au atom exchange which is observed in solution [11]. Suffice it to say that in the three new examples given here, the geometrical parameters are within the ranges considered in the earlier study. For example, the Au–Ru distances all fall near the A/C ends of the curve shown in Fig. 1 of Ref. [11].

4. Experimental

4.1. Instrumentation

IR: Perkin–Elmer 1700X FT IR; 683 double beam, NaCl optics; NMR: Bruker CXP300 or ACP300 (^{1}H NMR at 300.13 MHz, ^{13}C NMR at 75.47 MHz). FAB MS: VG ZAB 2HF (FAB MS, using 3-nitrobenzyl alcohol as matrix, exciting gas Ar, FAB gun voltage 7.5 kV, current 1 mA, accelerating potential 7 kV).

4.2. Starting materials

The compounds $[O\{Au(PPh_3)\}_3][BF_4]$ [32], [ppn][$Co(CO)_4$] [33], [ppn]Cl [33], [ppn][OAc] [34], $Os_3(CO)_{12}$ [35], $Ru_3(\mu_3\text{-}C_6H_4)(\mu\text{-}PPh_2)_2(CO)_7$ [36], $Ru_3(\mu_3\text{-}C_6H_3Me)\{\mu\text{-}P(C_6H_4Me\text{-}3)_2\}_2(CO)_7$ [36], $Ru_3\{\mu_3\text{-}PPhCH_2PPh(C_6H_4)\}(CO)_9$ [21b], $Ru_3(\mu_3\text{-}NPh)(CO)_{10}$ [22], $Ru_3(\mu_3\text{-}NPh)_2(CO)_9$ [37], $Ru_3(\mu_3\text{-}S)_2(CO)_9$ [38], $Ru_6C(CO)_{17}$ [39], $Os_3(CO)_{11}(NCMe)$ [40] and $Os_3(\mu\text{-}H)_2(CO)_{10}$ [41] were prepared by the cited methods.

4.2.1. $AuCl\{P(OMe)_3\}$

A modification of the method described in Ref. [42] was used. Au metal (2.01 g, 10.2 mmol) was dissolved in aqua regia (20 ml) in an evaporating dish, and then taken to dryness on a steam bath. The residue was then dissolved in HCl (10 ml) and again taken to dryness on the steam bath, redissolved in H_2O (20 ml) and filtered by gravity and the solution cooled in ice. Thiodiglycol (6 g, 49 mmol) was added to the filtrate dropwise over 1 h to give a clear solution. To this was added a solution of $P(OMe)_3$ (1.28 g, 10.3 mmol) in $CHCl_3$ (10 ml) dropwise over 20 min. The layers were separated and the water layer was washed with $CHCl_3$ (2 × 10 ml). The combined organic extracts were added to EtOH (100 ml) and evaporated (rotary evaporator) to approximately 10 ml to give $AuCl\{P(OMe)_3\}$ as a white powder (2.05 g, 56%), m.p. 98–101°C. IR (Nujol): ν(PO) 1180 cm^{-1}. ^{1}H NMR: $\delta(CDCl_3)$ 3.76 (d, J(PH) = 14.0 Hz, OMe). FAB MS (m/z): 677, $[\{Au[P(OMe)_3]\}_2Cl]^+$, 36; 445, $[Au\{P(OMe)_3\}_2]^+$, 12; 321, $[Au\{P(OMe)_3\}]^+$, 100.

4.2.2. $[O\{Au[P(OMe)_3]\}_3][BF_4]$

The brown precipitate of silver oxide formed by adding a solution of NaOH (0.45 g, 11 mmol) in H_2O (10 ml) to a solution of silver nitrate (1.88 g, 11.1 mmol) in H_2O (10 ml) was removed by filtration, washed with water (2 × 5 ml), ethanol (2.5 ml), and acetone (2 × 5 ml) and air dried. The solid silver oxide was then added to a round-bottomed, 250 ml flask containing a stirred solution of $AuCl\{P(OMe)_3\}$ in acetone (100 ml) (1.50 g, 4.21 mmol), followed by addition of solid $NaBF_4$ (1.88 g, 17.1 mmol). The mixture was stirred rapidly for 1 h. The solvent was removed and the solid residue was extracted with chloroform (3 × 15 ml). The combined extracts were filtered into freshly distilled Et_2O (150 ml) giving an off-white precipitate of $[O\{Au[P(OMe)_3]\}_3][BF_4]$ which was collected and air-dried (597 mg, 40%). Found: C, 10.21; H, 2.56; $C_9H_{27}Au_3BF_4O_{10}P_3$ requires C, 10.14; H, 2.55%. IR (Nujol): ν(PO) 1190 cm^{-1}; ν(BF) 1010–1080 (br) cm^{-1}. ^{1}H NMR: $\delta(CDCl_3)$ 3.82 (d, J(PH) = 13.4 Hz, OMe). FAB MS: 979, $[M]^+$; $[O\{Au[P(OMe)_3]\}_3]^+$, 100; 855, $[M - P(OMe)_3]^+$, 7: 839, $[M - P(OMe)_3 - O]^+$, 11; 659, $[M - Au\{P(OMe)_3\} + H]^+$, 22; 445, $[Au\{P(OMe)_3\}_2]^+$, 31; 321, $[Au\{P(OMe)_3\}]^+$, 69.

4.3. Reactions of osmium and ruthenium clusters with $[O\{Au(PR_3)\}_3][BF_4]$ (R = Ph, OMe) in the presence of $[ppn]^+$ salts

4.3.1. Preparation of $Ru_3(\mu_3\text{-}C_6H_4)(\mu\text{-}PPh_2)_2(CO)_6\{Au_2(PPh_3)_2\}$ (2)

To a stirred solution of $Ru_3(\mu_3\text{-}C_6H_4)(\mu\text{-}PPh_2)_2(CO)_7$ (14 mg, 0.015 mmol) in tetrahydrofuran (7 ml) were added $[O\{Au(PPh_3)\}_3][BF_4]$ (22 mg, 0.015 mmol) and [ppn][$Co(CO)_4$] (10 mg, 0.014 mmol). After 5 min the mixture was evaporated to dryness. Preparative TLC (acetone–light petroleum) gave five bands. Band 2 (colourless, R_f 0.56) contained $Co\{Au(PPh_3)\}(CO)_4$ IR: ν(CO) (cyclohexane) 2055s, 1990s, 1960vs cm^{-1} (Ref. [1a] ν(CO) (CS_2) 2054s, 1988s, 1957s cm^{-1}). FAB MS: 721, $[Au(PPh_3)_2]^+$, 28; 630, $[M]^+$, 2; 602, $[M - CO]^+$, 30; 574, $[M - 2CO]^+$, 14; 546, $[M - 3CO]^+$, 24; 518, $[M - 4CO]^+$, 34; 459, $[Au(PPh_3)]^+$, 100. Band 3 (purple, R_f 0.50) was crystallised (CH_2Cl_2–hexane) to give $Ru_3(\mu_3\text{-}C_6H_4)(\mu\text{-}PPh_2)_2(CO)_6\{Au_2(PPh_3)_2\}$ (**2**) (18 mg, 70%).

4.3.2. Preparation of $Ru_3(\mu_3\text{-}C_6H_3Me)\{\mu\text{-}P(C_6H_4Me\text{-}3)_2\}_2(CO)_6\{Au_2(PPh_3)_2\}$ (3)

In a similar reaction $[O\{Au(PPh_3)\}_3][BF_4]$ (36 mg, 0.024 mmol) and [ppn][$Co(CO)_4$] (17 mg, 0.024 mmol) were added to a solution of $Ru_3(\mu_3\text{-}C_6H_3Me)\{\mu\text{-}P(C_6H_4Me\text{-}3)_2\}_2(CO)_7$ (25 mg, 0.025 mmol) in tetrahydrofuran (10 ml). After 5 min the solvent was removed. Preparative TLC (acetone–light petroleum) gave six bands. Band 2 (colourless, R_f 0.61) contained $Co\{Au(PPh_3)\}(CO)_4$ (spot TLC), while band 3 (purple, R_f 0.54) was extracted and crystallised (CH_2Cl_2–hexane) to give $Ru_3(\mu_3\text{-}C_6H_3Me)\{\mu\text{-}P(C_6H_4Me\text{-}3)_2\}_2(CO)_6\{Au_2(PPh_3)_2\}$ (**3**) (33 mg, 72%). ^{1}H NMR: $\delta(CDCl_3)$ 1.87 (s, 3H, C_6H_3Me), 2.13 (s, 6H, C_6H_4Me-3), 2.18 (s, 6H, C_6H_4Me-3), 6.06–7.62 (m, 49H, C_6H_4Me-3 + C_6H_3Me + Ph).

4.3.3. Preparation of $Ru_3\{\mu_3\text{-}PPhCH_2PPh(C_6H_4)\}(CO)_8\{Au_2(PPh_3)_2\}$ (4)

4.3.3.1. From $[O\{Au(PPh_3)\}_3][BF_4]$–[ppn][$Co(CO)_4$]. — To a stirred solution of $Ru_3\{\mu_3\text{-}PPhCH_2PPh(C_6H_4)\}$

$(CO)_9$ (29 mg, 0.034 mmol) in tetrahydrofuran (10 ml) were added $[O\{Au(PPh_3)\}_3][BF_4]$ (52 mg, 0.035 mmol) and [ppn][$Co(CO)_4$] (26 mg, 0.037 mmol), immediately giving a purple solution. After stirring at room temperature for 15 min the solvent was removed. Preparative TLC (acetone–light petroleum) gave three bands. Band 1 (colourless, R_f 0.67) contained $Co\{Au(PPh_3)\}(CO)_4$ (IR ν(CO) spectrum and spot TLC). Band 3 (purple, R_f 0.53) was crystallised (CH_2Cl_2–MeOH) to give $Ru_3\{\mu_3\text{-}PPhCH_2PPh(C_6H_4)\}(CO)_8\{Au_2(PPh_3)_2\}$ (**4**) (47 mg, 79%). ^{1}H NMR: $\delta(CDCl_3)$ 2.83–2.95, 3.56–3.74 (2 × m, 2H, CH_2), 6.07–8.16 (m, 44H, Ph + C_6H_4).

4.3.3.2. From [O{Au(PPh$_3$)}$_3$][BF$_4$]–[ppn][OAc]. — A similar reaction of $Ru_3\{\mu_3\text{-}PPhCH_2PPh(C_6H_4)\}(CO)_9$ (23 mg, 0.027 mmol) with $[O\{Au(PPh_3)\}_3][BF_4]$ (40 mg, 0.027 mmol) and [ppn][OAc] (16 mg, 0.027 mmol) in tetrahydrofuran (8 ml) was stirred for 15 min, then evaporated to dryness. Preparative TLC (acetone–light petroleum 3/7) gave four bands. Band 3 (colourless, R_f 0.39) contained Au(OAc)(PPh_3) (spot TLC). Band 4 (purple, R_f 0.37) was crystallised (CH_2Cl_2–MeOH) to give feathery purple crystals of **4** (33 mg, 71%).

4.3.3.3. From [O{Au(PPh$_3$)}$_3$][BF$_4$]-[ppn]Cl. — Similarly, $[O\{Au(PPh_3)\}_3][BF_4]$ (57 mg, 0.039 mmol) and [ppn]Cl (22 mg, 0.038 mmol) were added to $Ru_3\{\mu_3\text{-}PPhCH_2PPh(C_6H_4)\}(CO)_9$ (33 mg, 0.038 mmol) in tetrahydrofuran (15 ml). After stirring for 10 min, and evaporation of the solvent, preparative TLC (acetone–light petroleum 3/7) gave six bands. Band 2 (red, R_f 0.82) contained unreacted $Ru_3\{\mu_3\text{-}PPhCH_2PPh(C_6H_4)\}(CO)_9$ (IR ν(CO) spectrum) (5 mg, 15%). Band 5 (colourless, R_f 0.64) contained $AuCl(PPh_3)$ (spot TLC) while band 6 (purple, R_f 0.54) was crystallised (CH_2Cl_2–MeOH) to give **4** (50 mg, 75%).

4.3.4. Preparation of Ru$_3${μ$_3$-PPhCH$_2$PPh(C$_6$H$_4$)}(CO)$_8${Au$_2$[P(OMe)$_3$]$_2$} (5)

To a stirred solution of $Ru_3\{\mu_3\text{-}PPhCH_2PPh(C_6H_4)\}(CO)_9$ (40 mg, 0.046 mmol) in tetrahydrofuran (12 ml) were added $[O\{Au[P(OMe)_3]\}_3][BF_4]$ (51 mg, 0.048 mmol) and [ppn][$Co(CO)_4$] (34 mg, 0.048 mmol). After stirring at room temperature for 5 min, the solvent was removed. Preparative TLC (acetone–light petroleum 3/7) of a CH_2Cl_2 extract gave one major band (purple, R_f 0.39) which was extracted and crystallised (CH_2Cl_2–MeOH) to give $Ru_3\{\mu_3\text{-}PPhCH_2PPh(C_6H_4)\}(CO)_8\{Au_2[P(OMe)_3]_2\}$ (**5**) (51 mg, 75%). ^{1}H NMR: $\delta(CDCl_3)$ 2.98–3.10, 3.61–3.75 (2 × m, 2H, CH_2), 3.55 (d, J(PH) 13.6Hz, 9H, OMe), 3.83 (d, J(PH) 13.3Hz, 9H, OMe), 6.03–8.12 (m, 14H, Ph + C_6H_4).

4.3.5. Preparation of Ru$_3$(μ$_3$-NPh)(CO)$_9${Au$_2$(PPh$_3$)$_2$} (6)

To a stirred solution of $Ru_3(\mu_3\text{-}NPh)(CO)_{10}$ (40 mg, 0.059 mmol) in tetrahydrofuran (15 ml) were added $[O\{Au(PPh_3)\}_3][BF_4]$ (89 mg, 0.060 mmol) and [ppn][$Co(CO)_4$] (42 mg, 0.059 mmol). After 15 min, solvent was removed and preparative TLC (acetone–light petroleum 3/7) separated six bands from a baseline. Band 2 (colourless, R_f 0.59) contained $Co\{Au(PPh_3)\}(CO)_4$ (IR ν(CO) spectrum and spot TLC). The major band (red, R_f 0.46) was extracted and crystallised (CH_2Cl_2–MeOH) to give $Ru_3(\mu_3\text{-}NPh)(CO)_9\{Au_2(PPh_3)_2\}$ (**6**) (60 mg, 65%). ^{1}H NMR: $\delta(CDCl_3)$ 7.31 (m, Ph).

4.3.6. Preparation of Ru$_3$(μ$_3$-NPh)$_2$(CO)$_8${Au$_2$(PPh$_3$)$_2$} (7)

To a stirred solution of $Ru_3(\mu_3\text{-}NPh)_2(CO)_9$ (42 mg, 0.057 mmol) in tetrahydrofuran (15 ml) were added $[O\{Au(PPh_3)\}_3][BF_4]$ (84 mg, 0.057 mmol) and [ppn][$Co(CO)_4$] (40 mg, 0.056 mmol). After stirring at room temperature for 5 min, the solvent was removed. Preparative TLC (acetone–light petroleum 3/7) gave two major bands and a brown baseline. Band 1 (colourless, R_f 0.67) contained $Co\{Au(PPh_3)\}(CO)_4$ (spot TLC). Band 2 (orange, R_f 0.55) was crystallised (CH_2Cl_2–MeOH) to give $Ru_3(\mu_3\text{-}NPh)_2(CO)_8\{Au_2(PPh_3)_2\}$ (**7**) (69 mg, 75%). ^{1}H NMR: $\delta(CDCl_3)$ 6.67–7.64 (m, Ph).

4.3.7. Preparation of Ru$_3$(μ$_3$-S)$_2$(CO)$_8${Au$_2$(PPh$_3$)$_2$} (8)

4.3.7.1. From [O{Au(PPh$_3$)}$_3$][BF$_4$]–[ppn][Co(CO)$_4$]. — As in 4.3.1. to a stirred solution of $Ru_3(\mu_3\text{-}S)_2(CO)_9$ (30 mg, 0.048 mmol) in tetrahydrofuran (10 ml) were added $[O\{Au(PPh_3)\}_3][BF_4]$ (72 mg, 0.049 mmol) and [ppn][$Co(CO)_4$] (35 mg, 0.049 mmol), resulting in an immediate darkening of the solution. After stirring at room temperature for 5 min the reaction mixture was evaporated to dryness. Preparative TLC (acetone–light petroleum 3/7) gave nine bands, seven of which were present in trace amounts and not identified. Band 2 (colourless, R_f 0.61) contained $Co\{Au(PPh_3)\}(CO)_4$ (spot TLC). Band 3 (orange, R_f 0.50) was crystallised (CH_2Cl_2–MeOH) to give $Ru_3(\mu_3\text{-}S)_2(CO)_8\{Au_2(PPh_3)_2\}$ (**8**) (50 mg, 69%). ^{1}H NMR: $\delta(CDCl_3)$ 7.48 (m, Ph).

4.3.7.2. From [O{Au(PPh$_3$)}$_3$][BF$_4$]–[ppn][OAc]. — A similar reaction of $Ru_3(\mu_3\text{-}S)_2(CO)_9$ (30 mg, 0.048 mmol) with $[O\{Au(PPh_3)\}_3][BF_4]$ (84 mg, 0.051 mmol) and [ppn][OAc] (31 mg, 0.052 mmol) in tetrahydrofuran (15 ml) was carried out for 5 min. After evaporation to dryness, preparative TLC gave one major orange band (R_f 0.59) which was crystallised (CH_2Cl_2–MeOH) to give **8** (41 mg, 57%).

4.3.7.3. From [O{Au(PPh$_3$)}$_3$][BF$_4$]–[ppn]Cl. — Similarly, a reaction between Ru$_3$(μ_3-S)$_2$(CO)$_9$ (36 mg, 0.058 mmol) with [O{Au(PPh$_3$)}$_3$][BF$_4$] (86 mg, 0.058 mmol) and [ppn]Cl (33 mg, 0.057 mmol) in tetrahydrofuran (13 ml) for 10 min gave four bands and a brown-red baseline (preparative TLC, acetone–light petroleum 3/7). Band 2 (orange, R_f 0.55) was crystallised (CH$_2$Cl$_2$–MeOH) to give **8** (18 mg, 21%).

4.3.8. Preparation of Ru$_6$C(μ-CO)$_2$(CO)$_{14}${Au(PPh$_3$)}$_2$ (9)

To a stirred solution of Ru$_6$C(CO)$_{17}$ (35 mg, 0.032 mmol) in tetrahydrofuran (15 ml) were added [O{Au(PPh$_3$)}$_3$][BF$_4$] (47 mg, 0.032 mmol) and [ppn][Co(CO)$_4$] (23 mg, 0.032 mmol). After stirring for 10 min the solvent was removed, and the residue was crystallised twice (CH$_2$Cl$_2$–MeOH) to give Ru$_6$C(μ-CO)$_2$(CO)$_{14}${Au(PPh$_3$)}$_2$ · 0.5CH$_2$Cl$_2$ (**9**) (30 mg, 47%).

4.3.9. Preparation of Os$_3$(CO)$_{11}${Au$_2$(PPh$_3$)$_2$} (10)

4.3.9.1. From [O{Au(PPh$_3$)}$_3$][BF$_4$]–[ppn][Co(CO)$_4$]. — To a stirred solution of Os$_3$(CO)$_{12}$ (22 mg, 0.024 mmol) in tetrahydrofuran (10 ml) were added [O{Au(PPh$_3$)}$_3$][BF$_4$] (36 mg, 0.024 mmol) and [ppn][Co(CO)$_4$] (17 mg, 0.024 mmol), all reactants dissolving within 5 min with a colour change from pale yellow to orange. After stirring at room temperature for 15 min, solvent was removed, diethyl ether (15 ml) was added and the volume was reduced; after cooling (−15°C), the resulting white precipitate was filtered off and identified (IR, FAB MS) as [ppn][BF$_4$] (12 mg, 80%). The filtrate was evaporated to dryness (rotary evaporator) and purified by preparative TLC (acetone–light petroleum 3/7) to give two major bands. Band 1 (colourless, R_f 0.54) was crystallised (CH$_2$Cl$_2$–MeOH) to give white crystals of Co{Au(PPh$_3$)}(CO)$_4$ (13 mg, 86%) (IR ν(CO) spectrum). Band 2 (orange, R_f 0.49) was crystallised (CH$_2$Cl$_2$–MeOH) to give Os$_3$(CO)$_{11}${Au$_2$(PPh$_3$)$_2$} (**10**) (30 mg, 70%). ^{1}H NMR: δ(CDCl$_3$) 7.30 (m, Ph).

4.3.9.2. From [O{Au(PPh$_3$)}$_3$][BF$_4$]–[ppn][OAc]. — In a similar reaction in which [O{Au(PPh$_3$)}$_3$][BF$_4$] (26 mg, 0.018 mmol) and [ppn][OAc] (10 mg, 0.017 mmol) were added to Os$_3$(CO)$_{12}$ (15 mg, 0.017 mmol) in tetrahydrofuran (10 ml), the mixture was stirred for 10 min and then evaporated to dryness in vacuo. Preparative TLC (acetone–light petroleum 3/7) gave two bands. Band 1 (orange, R_f 0.56) was crystallised (CH$_2$Cl$_2$–MeOH) to give **10** (21 mg, 71%), identified from its IR ν(CO) spectrum. Band 2 (colourless, R_f 0.48) was crystallised (CH$_2$Cl$_2$–MeOH) to give white crystals of Au(OAc)(PPh$_3$) (identified by comparison with an authentic sample).

4.3.9.3. From [O{Au(PPh$_3$)}$_3$][BF$_4$]–[ppn]Cl. — Similarly [O{Au(PPh$_3$)}$_3$][BF$_4$] (26 mg, 0.018 mmol) and [ppn]Cl (10 mg, 0.017 mmol) were added to

Table 7
Crystallographic data and refinement details for complexes **2**, **5**, **6** and **9**

Compound	**2**	**5**	**6**	**9**
Formula	$C_{72}H_{54}Au_2O_6P_4Ru_3$	$C_{33}H_{34}Au_2O_{14}P_4Ru_3 \cdot CH_2Cl_2$	$C_{51}H_{35}Au_2NO_9P_2Ru_3$	$C_{53}H_{30}Au_2O_{16}P_2Ru_6 \cdot 0.5CH_2Cl_2$
Formula wt.	1836.3	1560.6	1564.9	2027.6
Crystal size (mm^3)	0.11 × 0.23 × 0.48	0.13 × 0.46 × 0.51	0.16 × 0.26 × 0.33	0.06 × 0.06 × 0.31
Crystal system	monoclinic	monoclinic	monoclinic	monoclinic
Space group	$P2_1/c$	$P2_1/c$	$P2_1/c$	$P2_1/n$
a (Å)	22.924(3)	12.445(1)	13.615(3)	9.454(6)
b (Å)	14.245(4)	20.215(2)	21.224(3)	22.517(6)
c (Å)	25.631(4)	18.334(5)	18.653(5)	14.688(6)
β (deg)	112.85(1)	96.37(1)	108.60(2)	94.96(5)
V (Å^3)	7713.6	4583.9	5108.5	3114.9
D_{calcd} (g cm^{-3})	1.709	2.261	2.035	2.162
F(000)	3536	2944	2960	1898
Z	4	4	4	2
μ (cm^{-1})	50.65	75.88	66.50	62.77
Transmission coefficients	0.131–0.426	0.108–0.195	0.207–0.414	0.434–0.588
Data collected	$\pm h, +k, -l$	$-h, +k, \pm l$	$\pm h, +k, -l$	$\pm h, +k, -l$
No. of data	7815	7899	5911	2551
θ_{max}	20.0	22.5	21.0	20.0
No. of unique data ($I \geq 2.5\sigma(I)$)	3703	3711	3985	1389
R	0.088	0.051	0.040	0.041
k	1	0.86	1	3.8
g	0.015	0.006	0.003	0.0002
R_w	0.094	0.052	0.042	0.043
Residual density (e Å^{-3})	3.2 (near Au(2))	2.3 (near Au(2))	2.4 (near Au(1))	0.95

Table 8
Fractional atomic coordinates for $[Ru_3(\mu_3\text{-}C_6H_4)(\mu\text{-}PPh_2)_2(CO)_6\{Au_2(PPh_3)_2\}$ (**2**)

Atom	*x*	*y*	*z*
Au(1)	0.65795(7)	0.24234(9)	0.16661(7)
Au(2)	0.79708(7)	0.24954(8)	0.24363(6)
Ru(1)	0.7348(1)	0.4002(2)	0.1702(1)
Ru(2)	0.8205(1)	0.4581(2)	0.2794(1)
Ru(3)	0.7036(1)	0.3445(2)	0.2623(1)
P(1)	0.5917(5)	0.1411(6)	0.1015(5)
P(2)	0.8550(5)	0.1109(6)	0.2694(5)
P(3)	0.8310(4)	0.4731(5)	0.1925(4)
P(4)	0.7619(5)	0.4365(6)	0.3371(4)
O(11)	0.647(1)	0.484(2)	0.061(1)
O(12)	0.761(1)	0.263(2)	0.0962(10)
O(21)	0.938(1)	0.350(2)	0.345(1)
O(22)	0.884(1)	0.635(2)	0.338(1)
O(31)	0.733(1)	0.168(2)	0.339(1)
O(32)	0.572(2)	0.324(3)	0.259(2)
C(1)	0.678(1)	0.470(1)	0.2165(9)
C(2)	0.732(1)	0.526(1)	0.2286(9)
C(3)	0.726(1)	0.620(1)	0.2132(9)
C(4)	0.665(1)	0.659(1)	0.1858(9)
C(5)	0.612(1)	0.603(1)	0.1737(9)
C(6)	0.618(1)	0.509(1)	0.1890(9)
C(11)	0.684(2)	0.449(2)	0.103(1)
C(12)	0.752(2)	0.315(2)	0.129(2)
C(21)	0.895(2)	0.385(3)	0.318(2)
C(22)	0.863(2)	0.573(3)	0.311(2)
C(31)	0.728(2)	0.227(3)	0.305(2)
C(32)	0.619(3)	0.334(4)	0.261(3)
C(111)	0.520(1)	0.207(2)	0.057(1)
C(112)	0.525(1)	0.297(2)	0.037(1)
C(113)	0.472(1)	0.341(2)	−0.002(1)
C(114)	0.413(1)	0.296(2)	−0.021(1)
C(115)	0.408(1)	0.206(2)	−0.001(1)
C(116)	0.462(1)	0.162(2)	0.038(1)
C(121)	0.564(1)	0.044(1)	0.129(1)
C(122)	0.546(1)	0.062(1)	0.174(1)
C(123)	0.525(1)	−0.011(1)	0.199(1)
C(124)	0.522(1)	−0.102(1)	0.179(1)
C(125)	0.540(1)	−0.121(1)	0.134(1)
C(126)	0.561(1)	−0.048(1)	0.109(1)
C(131)	0.631(1)	0.087(2)	0.060(1)
C(132)	0.686(1)	0.035(2)	0.085(1)
C(133)	0.713(1)	−0.009(2)	0.051(1)
C(134)	0.685(1)	−0.001(2)	−0.007(1)
C(135)	0.629(1)	0.050(2)	−0.033(1)
C(136)	0.602(1)	0.094(2)	0.001(1)
C(211)	0.8070(9)	0.012(1)	0.2733(9)
C(212)	0.8384(9)	−0.069(1)	0.3013(9)
C(213)	0.8038(9)	−0.146(1)	0.3060(9)
C(214)	0.7378(9)	−0.144(1)	0.2826(9)
C(215)	0.7064(9)	−0.063(1)	0.2546(9)
C(216)	0.7410(9)	0.014(1)	0.2499(9)
C(221)	0.890(1)	0.071(1)	0.2208(8)
C(222)	0.946(1)	0.019(1)	0.2403(8)
C(223)	0.971(1)	−0.014(1)	0.2021(8)
C(224)	0.940(1)	0.004(1)	0.1444(8)
C(225)	0.884(1)	0.056(1)	0.1249(8)
C(226)	0.859(1)	0.089(1)	0.1630(8)
C(231)	0.916(1)	0.117(2)	0.3388(9)
C(232)	0.902(1)	0.092(2)	0.3849(9)
C(233)	0.947(1)	0.102(2)	0.4399(9)
C(234)	1.007(1)	0.138(2)	0.4487(9)
C(235)	1.021(1)	0.163(2)	0.4026(9)

Table 8 (continued)

Atom	x	y	z
C(236)	0.976(1)	0.152(2)	0.3477(9)
C(311)	0.8888(9)	0.415(1)	0.1701(9)
C(312)	0.9148(9)	0.331(1)	0.1969(9)
C(313)	0.9614(9)	0.285(1)	0.1840(9)
C(314)	0.9821(9)	0.324(1)	0.1442(9)
C(315)	0.9561(9)	0.408(1)	0.1173(9)
C(316)	0.9095(9)	0.453(1)	0.1303(9)
C(321)	0.837(1)	0.592(1)	0.167(1)
C(322)	0.882(1)	0.654(1)	0.202(1)
C(323)	0.883(1)	0.748(1)	0.186(1)
C(324)	0.839(1)	0.779(1)	0.134(1)
C(325)	0.793(1)	0.717(1)	0.099(1)
C(326)	0.793(1)	0.623(1)	0.115(1)
C(411)	0.798(2)	0.384(2)	0.405(1)
C(412)	0.753(2)	0.346(2)	0.423(1)
C(413)	0.772(2)	0.294(2)	0.473(1)
C(414)	0.837(2)	0.281(2)	0.505(1)
C(415)	0.882(2)	0.319(2)	0.487(1)
C(416)	0.862(2)	0.371(2)	0.437(1)
C(421)	0.729(2)	0.544(2)	0.352(1)
C(422)	0.769(2)	0.602(2)	0.394(1)
C(423)	0.745(2)	0.680(2)	0.412(1)
C(424)	0.681(2)	0.700(2)	0.388(1)
C(425)	0.640(2)	0.641(2)	0.346(1)
C(426)	0.664(2)	0.563(2)	0.328(1)

$Os_3(CO)_{12}$ (15 mg, 0.017 mmol) in tetrahydrofuran (10 ml). After stirring for 10 min and evaporation of the solvent, preparative TLC (acetone–light petroleum 3/7) gave three bands. Band 1 (yellow, R_f 0.83) (trace) was identified as unreacted $Os_3(CO)_{12}$ (IR ν(CO) spectrum); band 2 (orange, R_f 0.48) was crystallised (CH_2Cl_2–MeOH) to give **10** (16 mg, 54%), identified from its IR ν(CO) spectrum; band 3 (colourless, R_f 0.42) was crystallised ($CHCl_3$–EtOH) to give white crystals of $AuCl(PPh_3)$ (identified by comparison with an authentic sample).

4.3.10. Preparation of $Os_3(CO)_{11}\{Au_2[P(OMe)_3]_2\}$ (11)

As in 4.3.9, to a stirred solution of $Os_3(CO)_{12}$ (29 mg, 0.032 mmol) in tetrahydrofuran (15 ml) were added $[O\{Au[P(OMe)_3]\}_3][BF_4]$ (34 mg, 0.0.32 mmol) and $[ppn][Co(CO)_4]$ (23 mg, 0.032 mmol) giving an immediate colour change from pale yellow to orange. After evaporation to dryness, preparative TLC (acetone–light petroleum 3/7) showed one major band (orange, R_f 0.50), which was extracted and crystallised (CH_2Cl_2–MeOH) to give $Os_3(CO)_{11}\{Au_2[P(OMe)_3]_2\}$ (**11**) (26 mg, 53%). ^{1}H NMR: $\delta(CDCl_3)$ 3.79 (d, J(PH) 13.5 Hz, OMe).

4.3.11. Preparation of $Os_3(CO)_{10}\{Au(PPh_3)\}_2$ (12)

Similarly, to a stirred solution of $Os_3(CO)_{11}(NCMe)$ (42 mg, 0.046 mmol) in tetrahydrofuran (17 ml) were added $[O\{Au(PPh_3)\}_3][BF_4]$ (68 mg, 0.046 mmol) and $[ppn][Co(CO)_4]$ (32 mg, 0.045 mmol). The colour of the solution changed immediately from yellow to yellow green, all reactants having dissolved after about 15 min. After 1.5 h at room temperature, the solution was dark green. After evaporation to dryness, preparative TLC (acetone–light petroleum 3/7) separated seven bands from a red-brown baseline. Band 2 (colourless, R_f 0.63) contained $Co\{Au(PPh_3)\}(CO)_4$ (IR ν(CO) spectrum and spot TLC). Band 3 (green, R_f 0.57) was crystallised (CH_2Cl_2–MeOH) to give $Os_3(CO)_{10}\{Au(PPh_3)\}_2$ (**12**) (33 mg, 51%).

4.3.12. Reaction between $Os_3(\mu\text{-}H)_2(CO)_{10}$ and $[O\{Au(PPh_3)\}_3][BF_4]$–[ppn][Co(CO)$_4$]

A mixture of $[O\{Au(PPh_3)\}_3][BF_4]$ (110 mg, 0.074 mmol) and $[ppn][Co(CO)_4]$ (53 mg, 0.075 mmol) was added to a solution of $Os_3(\mu\text{-}H)_2(CO)_{10}$ (63 mg, 0.074 mmol) in tetrahydrofuran (20 ml) giving an immediate colour change from purple to green-brown. After stirring for 7 min the solvent was removed. Preparative TLC (acetone–light petroleum 3/7) gave seven bands and a brown baseline. Band 1 (green, R_f 0.60) was crystallised (CH_2Cl_2–MePh) to give $Os_3(\mu\text{-}H)(CO)_{10}\{Au(PPh_3)\}$ (**13**) (15 mg, 15%). Band 3 (green-yellow, R_f 0.43) was crystallised (CH_2Cl_2–MeOH) to give $Os_3(CO)_{10}\{Au(PPh_3)\}_2$ (**12**) (21 mg, 16%) (IR ν(CO) spectrum and spot TLC). Band 5 (yellow, R_f 0.31) was crystallised (CH_2Cl_2–MeOH) to give $Os_3(\mu\text{-}H)_2(CO)_9(PPh_3)\{Au(PPh_3)\}_2$ (**14**) (12 mg, 8%). ^{1}H NMR: Δ ($CDCl_3$) −17.04 (t, J(PH) 15 Hz, 1H, Ru–H), −7.01 (d, J(PH) 12 Hz, 1H, Ru–H), 7.16–7.47 (m, 45H, Ph).

Table 9
Fractional atomic coordinates for $Ru_3\{\mu_3\text{-}PPhCH_2PPh(C_6H_4\text{-}2)\}(CO)_8\{Au_2(P(OMe)_3)_2\} \cdot CH_2Cl_2$ (5)

Atom	x	y	z
Au(1)	0.39160(6)	0.13315(3)	0.26250(3)
Au(2)	0.39667(5)	0.23293(3)	0.36580(4)
Ru(1)	0.1927(1)	0.19233(6)	0.29010(6)
Ru(2)	0.1894(1)	0.23327(6)	0.44229(6)
Ru(3)	0.32118(9)	0.11248(6)	0.40635(6)
Cl(1)	0.8663(9)	0.4964(6)	0.5380(7)
Cl(2)	0.8817(9)	0.3936(6)	0.6462(9)
P(1)	0.5012(4)	0.0925(2)	0.1825(3)
P(2)	0.5409(4)	0.3009(3)	0.3731(3)
P(3)	0.1568(3)	0.0893(2)	0.3390(2)
P(4)	0.0956(3)	0.1367(2)	0.4752(2)
O(11)	−0.040(1)	0.2334(7)	0.3089(7)
O(12)	0.141(1)	0.1468(7)	0.1332(7)
O(13)	0.245(1)	0.3301(6)	0.2332(7)
O(21)	0.270(1)	0.3697(6)	0.4025(7)
O(22)	0.328(1)	0.2305(7)	0.5880(7)
O(23)	−0.006(1)	0.3149(7)	0.4695(8)
O(31)	0.4120(9)	−0.0178(6)	0.3692(7)
O(32)	0.522(1)	0.1470(6)	0.5082(7)
O(111)	0.565(1)	0.0330(7)	0.2131(7)
O(112)	0.584(2)	0.1371(8)	0.156(1)
O(113)	0.451(2)	0.064(1)	0.1105(9)
O(211)	0.653(1)	0.2718(8)	0.3503(9)
O(212)	0.533(1)	0.3674(7)	0.3273(10)
O(213)	0.560(2)	0.332(1)	0.4547(9)
C(1)	0.181(1)	0.0798(7)	0.5287(7)
C(2)	0.279(1)	0.0654(6)	0.5009(7)
C(3)	0.349(1)	0.0189(7)	0.5412(8)
C(4)	0.320(1)	−0.0058(8)	0.6074(9)
C(5)	0.228(1)	0.0101(8)	0.6357(8)
C(6)	0.158(1)	0.0545(7)	0.5956(8)
C(11)	0.050(2)	0.2226(9)	0.310(1)
C(12)	0.164(1)	0.1638(8)	0.1945(9)
C(13)	0.235(2)	0.2772(9)	0.2571(9)
C(21)	0.249(2)	0.3156(8)	0.4146(9)
C(22)	0.278(1)	0.2283(7)	0.5317(9)
C(23)	0.069(2)	0.2847(10)	0.4591(10)
C(31)	0.379(1)	0.0323(8)	0.3802(8)
C(32)	0.450(1)	0.1405(7)	0.4648(9)
C(100)	0.943(2)	0.445(1)	0.590(2)
C(111)	0.641(2)	−0.006(1)	0.172(1)
C(112)	0.595(3)	0.203(2)	0.153(2)
C(113)	0.361(2)	0.074(2)	0.064(2)
C(211)	0.695(3)	0.208(2)	0.367(2)
C(212)	0.515(2)	0.363(1)	0.244(1)
C(213)[2]	0.648(4)	0.384(2)	0.477(2)
C(213′) [a]	0.712(6)	0.343(3)	0.479(4)
C(331)	0.1320(7)	0.0170(6)	0.2778(6)
C(332)	0.0325(7)	−0.0154(6)	0.2716(6)
C(333)	0.0152(7)	−0.0705(6)	0.2261(6)
C(334)	0.0975(7)	−0.0932(6)	0.1867(6)
C(335)	0.1970(7)	−0.0608(6)	0.1928(6)
C(336)	0.2143(7)	−0.0057(6)	0.2383(6)
C(341)	0.045(1)	0.0868(7)	0.3968(7)
C(411)	−0.0199(8)	0.1487(5)	0.5266(5)
C(412)	−0.1123(8)	0.1094(5)	0.5143(5)
C(413)	−0.1942(8)	0.1150(5)	0.5601(5)
C(414)	−0.1837(8)	0.1599(5)	0.6182(5)
C(415)	−0.0914(8)	0.1992(5)	0.6306(5)
C(416)	−0.0095(8)	0.1937(5)	0.5848(5)

[a] Atom has 50% site occupancy.

Table 10
Fractional atomic coordinates for $Ru_3(\mu_3\text{-NPh})(CO)_9\{Au_2(PPh_3)_2\}$ (6)

Atom	x	y	z
Au(1)	0.10371(4)	−0.18540(2)	0.30955(3)
Au(2)	0.26410(4)	−0.12269(2)	0.25920(3)
Ru(1)	0.30623(7)	−0.23016(4)	0.36386(5)
Ru(2)	0.40058(7)	−0.22057(4)	0.25526(6)
Ru(3)	0.18508(7)	−0.24292(4)	0.20494(5)
P(1)	−0.0430(2)	−0.1474(2)	0.3305(2)
P(2)	0.2472(2)	−0.0176(1)	0.2256(2)
O(11)	0.1923(8)	−0.3027(4)	0.4552(6)
O(12)	0.3261(7)	−0.1124(5)	0.4617(6)
O(13)	0.5172(8)	−0.2698(5)	0.4660(6)
O(21)	0.6085(8)	−0.2868(5)	0.3183(7)
O(22)	0.4015(8)	−0.2268(6)	0.0935(6)
O(23)	0.5213(8)	−0.0976(5)	0.2908(8)
O(31)	0.0041(9)	−0.3224(5)	0.2151(7)
O(32)	0.1847(8)	−0.3121(5)	0.0631(6)
O(33)	0.0498(8)	−0.1418(5)	0.1032(6)
N(1)	0.3090(7)	−0.2908(4)	0.2767(5)
C(1)	0.3289(6)	−0.3575(3)	0.2788(4)
C(2)	0.3067(6)	−0.3957(3)	0.3325(4)
C(3)	0.3245(6)	−0.4605(3)	0.3329(4)
C(4)	0.3644(6)	−0.4870(3)	0.2796(4)
C(5)	0.3866(6)	−0.4488(3)	0.2259(4)
C(6)	0.3688(6)	−0.3840(3)	0.2255(4)
C(11)	0.228(1)	−0.2750(6)	0.4177(7)
C(12)	0.3158(10)	−0.1547(6)	0.4227(7)
C(13)	0.439(1)	−0.2546(6)	0.4255(8)
C(21)	0.529(1)	−0.2629(6)	0.2970(8)
C(22)	0.397(1)	−0.2261(7)	0.1536(9)
C(23)	0.470(1)	−0.1407(6)	0.2738(9)
C(31)	0.0733(10)	−0.2912(6)	0.2141(7)
C(32)	0.1906(10)	−0.2855(6)	0.1158(8)
C(33)	0.100(1)	−0.1779(6)	0.1444(8)
C(111)	−0.0901(8)	−0.1912(5)	0.3954(5)
C(112)	−0.1495(8)	−0.1609(5)	0.4337(5)
C(113)	−0.1901(8)	−0.1952(5)	0.4816(5)
C(114)	−0.1713(8)	−0.2597(5)	0.4911(5)
C(115)	−0.1119(8)	−0.2900(5)	0.4529(5)
C(116)	−0.0713(8)	−0.2557(5)	0.4050(5)
C(121)	−0.0287(6)	−0.0668(3)	0.3633(5)
C(122)	0.0695(6)	−0.0469(3)	0.4078(5)
C(123)	0.0847(6)	0.0151(3)	0.4340(5)
C(124)	0.0018(6)	0.0572(3)	0.4155(5)
C(125)	−0.0964(6)	0.0373(3)	0.3710(5)
C(126)	−0.1116(6)	−0.0246(3)	0.3449(5)
C(131)	−0.1530(5)	−0.1460(4)	0.2441(4)
C(132)	−0.2479(5)	−0.1735(4)	0.2393(4)
C(133)	−0.3296(5)	−0.1716(4)	0.1714(4)
C(134)	−0.3164(5)	−0.1420(4)	0.1083(4)
C(135)	−0.2215(5)	−0.1145(4)	0.1131(4)
C(136)	−0.1398(5)	−0.1164(4)	0.1810(4)
C(211)	0.3159(6)	−0.0021(4)	0.1578(4)
C(212)	0.3513(6)	0.0582(4)	0.1488(4)
C(213)	0.3936(6)	0.0699(4)	0.0912(4)
C(214)	0.4006(6)	0.0214(4)	0.0425(4)
C(215)	0.3652(6)	−0.0388(4)	0.0516(4)
C(216)	0.3229(6)	−0.0506(4)	0.1092(4)
C(221)	0.1183(5)	0.0114(4)	0.1778(5)
C(222)	0.0877(5)	0.0302(4)	0.1022(5)
C(223)	−0.0123(5)	0.0530(4)	0.0676(5)
C(224)	−0.0817(5)	0.0571(4)	0.1086(5)
C(225)	−0.0511(5)	0.0383(4)	0.1842(5)
C(226)	0.0489(5)	0.0154(4)	0.2188(5)

Table 10 (continued)

Atom	x	y	z
C(231)	0.3009(6)	0.0398(4)	0.3012(5)
C(232)	0.3875(6)	0.0217(4)	0.3611(5)
C(233)	0.4361(6)	0.0649(4)	0.4176(5)
C(234)	0.3981(6)	0.1263(4)	0.4142(5)
C(235)	0.3116(6)	0.1444(4)	0.3543(5)
C(236)	0.2630(6)	0.1012(4)	0.2978(5)

5. Crystallography

Intensity data for **2**, **5**, **6** and **9** were measured at room temperature on an Enraf–Nonius CAD4F diffractometer fitted with Mo Kα radiation (λ 0.7107 Å) employing the ω–2θ scan technique. Corrections were applied for absorption effects and only those data which satisfied the $I \geq 2.5\sigma(I)$ criterion were employed in the analysis. Crystal data are given in Table 7. The structures were each solved by direct-methods [43] and

Table 11
Fractional atomic coordinates for $Ru_6C(\mu\text{-}CO)_2(CO)_{14}\{Au(PPh_3)\}_2 \cdot 0.5CH_2Cl_2$ (**9**)

Atom	x	y	z
Au(1)	0.33954(9)	−0.14431(4)	0.42311(8)
Ru(1)	0.5504(2)	−0.06046(7)	0.4012(2)
Ru(2)	0.3372(2)	−0.05133(7)	0.5446(2)
Ru(3)	0.6362(2)	−0.03908(7)	0.5957(2)
P(1)	0.2230(6)	−0.2251(3)	0.3602(5)
O(11)	0.768(2)	−0.0051(7)	0.287(1)
O(12)	0.728(2)	−0.1700(8)	0.370(1)
O(13)	0.404(2)	−0.0790(7)	0.213(2)
O(21)	0.359(2)	−0.1612(7)	0.661(1)
O(22)	0.022(2)	−0.0726(7)	0.505(1)
O(31)	0.911(2)	0.0138(7)	0.681(1)
O(32)	0.786(2)	−0.1572(8)	0.574(1)
O(33)	0.552(2)	−0.0693(7)	0.781(2)
C(1) [a]	0.5	0	0.5
C(11)	0.702(3)	−0.005(1)	0.351(2)
C(12)	0.657(3)	−0.128(1)	0.383(2)
C(13)	0.457(2)	−0.0743(9)	0.286(2)
C(21)	0.343(2)	−0.1211(10)	0.612(2)
C(22)	0.142(3)	−0.0644(10)	0.520(2)
C(31)	0.806(3)	−0.006(1)	0.642(2)
C(32)	0.726(3)	−0.112(1)	0.578(2)
C(33)	0.590(3)	−0.058(1)	0.709(2)
C(111)	0.343(2)	−0.2832(6)	0.332(1)
C(112)	0.460(2)	−0.2673(6)	0.291(1)
C(113)	0.556(2)	−0.3131(6)	0.265(1)
C(114)	0.531(2)	−0.3707(6)	0.283(1)
C(115)	0.414(2)	−0.3870(6)	0.322(1)
C(116)	0.321(2)	−0.3447(6)	0.350(1)
C(121)	0.119(2)	−0.2026(7)	0.257(1)
C(122)	0.033(2)	−0.1525(7)	0.259(1)
C(123)	−0.041(2)	−0.1320(7)	0.179(1)
C(124)	−0.028(2)	−0.1616(7)	0.097(1)
C(125)	0.058(2)	−0.2117(7)	0.095(1)
C(126)	0.132(2)	−0.2323(7)	0.175(1)
C(131)	0.097(2)	−0.2604(6)	0.428(1)
C(132)	−0.032(2)	−0.2832(6)	0.390(1)
C(133)	−0.119(2)	−0.3145(6)	0.445(1)
C(134)	−0.078(2)	−0.3230(6)	0.538(1)
C(135)	0.051(2)	−0.3003(6)	0.576(1)
C(136)	0.139(2)	−0.2690(6)	0.521(1)
Cl(1) [a]	0.351(3)	0.048(1)	0.965(2)
Cl(2) [a]	0.165(4)	−0.033(1)	1.014(2)
C(2) [a]	0.315(10)	−0.016(4)	0.952(7)

[a] Atom has 50% site occupancy.

refined by a full-matrix least squares procedure based on F [43]. Anisotropic thermal parameters were employed (**2**: Au, Ru, P; **5**: non-H; **6**: non-H, non-phenyl; **9**: Au, Ru, P) and H atoms were included in their calculated positions except for the refinement of **9**. After the inclusion of a weighting scheme of the form $k/[\sigma^2(F) + gF^2]$, the refinements were continued until convergence; final refinement details are given in Table 7. Fractional atomic coordinates are listed in Tables 8 to 11 and the numbering schemes employed are shown in Figs. 1 to 4 which were drawn at 25% probability ellipsoids with the ORTEP program [44]. Scattering factors (corrected for f' and f'') were those incorporated in SHELX76 or from Ref. [45]. H-atom parameters, a complete list of bond distances and angles, and thermal parameters have been deposited at the Cambridge Crystallographic Data Centre.

Acknowledgments

Financial support from the Australian Research Council is gratefully acknowledged. Johnson Matthey Technology is thanked for generous loans of $RuCl_3 \cdot nH_2O$ and OsO_4. PAH was the holder of a University of Adelaide Postgraduate Scholarship. We thank a referee for some helpful comments.

References

[1] (a) C.E. Coffey, J. Lewis and R.S. Nyholm, *J. Chem. Soc.*, (1964) 1741; (b) A.S. Kasenally, R.S. Nyholm and R.J. O'Brien, *Nature, 204* (1964) 871; (c) A.S. Kasenally, R.S. Nyholm and M.H.B. Stiddard, *J. Am. Chem. Soc., 86* (1964) 1884.
[2] J.W. Lauher and K. Wald, *J. Am. Chem. Soc., 103* (1981) 7648.
[3] K.P. Hall and D.M.P. Mingos, *Prog. Inorg. Chem., 32* (1984) 237.
[4] B.K. Teo, M. Hong, H. Zhang, D. Huang and X. Shi, *J. Chem. Soc. Chem. Commun.*, (1988) 204.
[5] (a) P. Braunstein and J. Rosé, *Gold Bull., 18* (1985) 17; (b) A.M. Mueting, W. Bos, B.D. Alexander, P.D. Boyle, J.A. Casalnuovo, S. Balaban, L.N. Ito, S.M. Johnson and L.H. Pignolet, *New J. Chem., 12* (1988) 505; (c) I.D. Salter, *Adv. Organomet. Chem., 29* (1989) 249; (d) D.M.P. Mingos and M.J. Watson, *Adv. Inorg. Chem., 39* (1992) 327.
[6] (a) M.I. Bruce and B.K. Nicholson, *J. Chem. Soc. Chem. Commun.*, (1982) 1141; (b) M.I. Bruce and B.K. Nicholson, *Organometallics, 3* (1984) 1101.
[7] (a) K.S. Harpp, C.E. Housecroft, A.L. Rheingold and M.S. Shongwe, *J. Chem. Soc. Chem. Commun.*, (1988) 965; (b) V. Dearing, S.R. Drake, B.F.G. Johnson, J. Lewis, M. McPartlin and H.R. Powell, *J. Chem. Soc. Chem. Commun.*, (1988) 1331.
[8] M.I. Bruce, P.E. Corbin, P.A. Humphrey, G.A. Koutsantonis, M.J. Liddell and E.R.T. Tiekink, *J. Chem. Soc. Chem. Commun.*, (1990) 674.
[9] M.I. Bruce, P.A. Humphrey, B.W. Skelton and A.H. White, in preparation.
[10] I.D. Salter, *Adv. Dynamic Stereochem., 2* (1988) 57.
[11] A.G. Orpen and I.D. Salter, *Organometallics, 10* (1991) 111.
[12] (a) T. Blumenthal, M.I. Bruce, O. bin Shawkataly, B.N. Green and I. Lewis, *J. Organomet. Chem., 269* (1984) C10; (b) M.I. Bruce and M.J. Liddell, *J. Organomet. Chem., 427* (1992) 263.
[13] (a) L.J. Farrugia, M.J. Freeman, M. Green, A.G. Orpen, F.G.A. Stone and I.D. Salter, *J. Organomet. Chem., 249* (1983) 273; (b) M.I. Bruce, O. bin Shawkataly and B.K. Nicholson, *J. Organomet. Chem., 286* (1985) 427.
[14] S.R. Bunkhall, H.D. Holden, B.F.G. Johnson, J. Lewis, G.N. Pain, P.R. Raithby and M.J. Taylor, *J. Chem. Soc. Chem. Commun.*, (1984) 25.
[15] K. Burgess, B.F.G. Johnson, D.A. Kaner, J. Lewis, P.R. Raithby and S.N.A.B. Syed-Mustaffa, *J. Chem. Soc. Chem. Commun.*, (1983) 455.
[16] J.A.K. Howard, L.J. Farrugia, C. Foster, F.G.A. Stone and P. Woodward, *Eur. Cryst. Mtg., 6* (1980) 73.
[17] L.J. Farrugia, J.A.K. Howard, P. Mitrprachachon, J.L. Spencer, F.G.A. Stone and P. Woodward, *J. Chem. Soc. Chem. Commun.*, (1978) 260.
[18] B.F.G. Johnson, D.A. Kaner, J. Lewis and P.R. Raithby, *J. Organomet. Chem., 215* (1981) C33.
[19] J.R. Shapley, J.B. Keister, M.R. Churchill and B.G. DeBoer, *J. Am. Chem. Soc., 97* (1975) 4145.
[20] M.I. Bruce, J.M. Guss, R. Mason, B.W. Skelton and A.H. White, *J. Organomet. Chem., 251* (1983) 261.
[21] (a) N. Lugan, J.-J. Bonnet and J.A. Ibers, *J. Am. Chem. Soc., 107* (1985) 4484; (b) M.I. Bruce, P.A. Humphrey, M.L. Williams, B.W. Skelton and A.H. White, *Aust. J. Chem., 38* (1985) 1301.
[22] S. Bhaduri, K.S. Gopalkrishnan, G.M. Sheldrick, W. Clegg and D. Stalke, *J. Chem. Soc. Dalton Trans.*, (1983) 2339.
[23] D. Braga, F. Grepioni, P.J. Dyson, B.F.G. Johnson, P. Frediani, M. Bianchi and F. Piacenti, *J. Chem. Soc. Dalton Trans.*, (1992) 2565.
[24] M.I. Bruce, M.L. Williams, J.M. Patrick, B.W. Skelton and A.H. White, *J. Chem. Soc. Dalton Trans.*, (1986) 2557.
[25] M.J. Freeman, A.G. Orpen and I.D. Salter, *J. Chem. Soc. Dalton Trans.*, (1987) 379.
[26] S.A.R. Knox, B.R. Lloyd, D.A.V. Morton, S.M. Nicholls, A.G. Orpen, J.M. Viñas, M. Weber and G.K. Williams, *J. Organomet. Chem., 394* (1990) 385.
[27] B.F.G. Johnson, D.A. Kaner, J. Lewis, P.R. Raithby and M.J. Taylor, *Polyhedron, 1* (1982) 105.
[28] H. Schmidbaur, *Gold Bull., 23* (1990) 11; *Pure Appl. Chem., 65* (1993) 691.
[29] P.J. Bailey, M.A. Beswick, J. Lewis, P.R. Raithby and M.A. Ramirez de Arellano, *J. Organomet. Chem., 459* (1993) 293.
[30] J.W. Lauher and K. Wald, *J. Am. Chem. Soc., 103* (1981) 7648.
[31] G.J. Kubas, R.R. Ryan, B.I. Swanson, P.J. Vergamini and H.J. Wassermann, *J. Am. Chem. Soc., 106* (1984) 451. See also the recent reviews: D.M. Heinekey, *Chem. Rev., 93* (1993) 913; R.H. Morris and P.G. Jessop, *Coord. Chem. Rev., 121* (1992) 155; A. Dedieu (ed.), *Transition Metal Hydrides* VCH, Weinheim, 1991.
[32] (a) A.N. Nesmeyanov, E.G. Perevalova, Yu.T. Struchkov, M.Yu. Antipin, K.I. Grandberg and V.P. Dyadchenko, *J. Organomet. Chem., 201* (1980) 343; (b) M.I. Bruce, B.K. Nicholson and O. bin Shawkataly, *Inorg. Synth., 26* (1989) 324.
[33] J.K. Ruff and W.J. Schlientz, *Inorg. Synth., 15* (1974) 84.
[34] A. Martinson and J. Songstad, *Acta Chem. Scand. A, 31* (1977) 645.
[35] S.R. Drake and P.A. Loveday, *Inorg. Synth., 28* (1990) 230.
[36] M.I. Bruce, G. Shaw and F.G.A. Stone, *J. Chem. Soc. Dalton Trans.*, (1972) 2094.
[37] M.I. Bruce, M.G. Humphrey, O. bin Shawkataly, M.R. Snow and E.R.T. Tiekink, *J. Organomet. Chem., 336* (1987) 199.
[38] R.D. Adams, J.E. Babin and M. Tasi, *Inorg. Chem., 25* (1986) 4514.

[39] J.N. Nicholls and M.D. Vargas, *Inorg. Synth., 26* (1989) 280.
[40] J.N. Nicholls and M.D. Varga, *Inorg. Synth., 28* (1990) 232.
[41] (a) S.A.R. Knox, J.W. Koepke, M.A. Andrews and H.D. Haesz, *J. Am. Chem. Soc., 97* (1975) 3942; (b) H.D. Kaesz, *Inorg. Synth., 28* (1990) 238.
[42] A.K. Al-Sa'ady, C.A. McAuliffe, R.V. Parish and J.A. Sandbank, *Inorg. Synth., 23* (1985) 191.
[43] G.M. Sheldrick, SHELX76, *Program for crystal structure determination*, University of Cambridge, 1976.
[44] C.K. Johnson, ORTEPII, *Rep. ORNL-3794*, (Oak Ridge National Laboratory, Oak Ridge, TN).
[45] J.A. Ibers and W.C. Hamilton (eds.), *International Tables for X-Ray Crystallography*, Vol. 4, Kynoch Press, Birmingham, 1974, p. 99; 149.